

# Gearing up for the next generation of LFV experiments, via on-shell methods

Joan Elias Miró,<sup>a</sup> Clara Fernandez,<sup>d</sup> Mehmet Asım Gümüş<sup>b,c</sup> and Alex Pomarol<sup>d,e</sup>

<sup>a</sup>*ICTP, International Centre for Theoretical Physics,  
Strada Costiera 11, I-34151, Trieste, Italy*

<sup>b</sup>*SISSA,  
Via Bonomea 265, I-34136 Trieste, Italy*

<sup>c</sup>*INFN, Sezione di Trieste,  
Via Valerio 2, I-34127 Trieste, Italy*

<sup>d</sup>*IFAE and BIST, Universitat Autònoma de Barcelona,  
08193 Bellaterra, Barcelona*

<sup>e</sup>*Departament de Física, Universitat Autònoma de Barcelona,  
08193 Bellaterra, Barcelona*

*E-mail:* [joaneliasmiro@gmail.com](mailto:joaneliasmiro@gmail.com), [cfernandez@ifae.es](mailto:cfernandez@ifae.es), [mgumus@ictp.it](mailto:mgumus@ictp.it),  
[alex.pomarol@uab.cat](mailto:alex.pomarol@uab.cat)

**ABSTRACT:** Lepton Flavor Violating (LFV) observables such as  $\mu \rightarrow e\gamma$ ,  $\mu \rightarrow 3e$  and  $\mu N \rightarrow eN$  are among the best probes for new physics at the TeV scale. In the near future the bounds on these observables will improve by many orders of magnitude. In this work we use the SM EFT to understand the impact of these measurements. The precision reach is such that the interpretation of the bounds requires an analysis of the dimension-six operator mixing up to the two-loop level. Using on-shell amplitude techniques, which make transparent many selection rules, we classify and calculate the different operator mixing chains. At the leading order, on-shell techniques allow to calculate anomalous dimensions of SM EFT operators from the product of tree-level amplitudes, even for two-loop renormalization group mixings. We illustrate the importance of our EFT approach in models with extra vector-like fermions.

**KEYWORDS:** Effective Field Theories, Lepton Flavour Violation (charged), Scattering Amplitudes

ARXIV EPRINT: [2112.12131](https://arxiv.org/abs/2112.12131)

---

## Contents

<b>1</b>	<b>Introduction</b>	<b>1</b>
<b>2</b>	<b>LFV dimension-six operator basis</b>	<b>3</b>
2.1	LFV experimental constraints at the tree level	4
<b>3</b>	<b><math>\mu \rightarrow e\gamma</math> in the SM EFT</b>	<b>7</b>
<b>4</b>	<b>The on-shell way</b>	<b>8</b>
4.1	One-loop mixing into LFV dipoles	9
4.2	Two-loop mixing into dipoles	11
4.2.1	Top Yukawa $y_t^2$ contributions	12
4.2.2	Higgs quartic $\lambda$ contributions	14
4.3	Finite one-loop contributions at the electroweak scale	16
<b>5</b>	<b><math>\mu \rightarrow eee</math> in the SM EFT</b>	<b>17</b>
<b>6</b>	<b><math>\mu N \rightarrow eN</math> in the SM EFT</b>	<b>17</b>
<b>7</b>	<b>Constraints from anomalous dimension mixings</b>	<b>18</b>
<b>8</b>	<b>Impact on UV models</b>	<b>19</b>
8.1	Heavy vector-like fermions	20
8.2	BSM with lepton universality violations	21
<b>9</b>	<b>Conclusions</b>	<b>22</b>
<b>A</b>	<b>One-loop anomalous dimensions relevant for LFV</b>	<b>23</b>
A.1	$\mu \rightarrow e\gamma$	23
A.2	$\mu \rightarrow eee$	24
A.3	$\mu N \rightarrow eN$	25
<b>B</b>	<b>Conventions and minimal form factors</b>	<b>25</b>
<b>C</b>	<b>Tensors</b>	<b>26</b>

---

## 1 Introduction

In the SM, lepton numbers  $L_{e,\mu,\tau}$  arise from accidental symmetries that guarantee the absence of neutrino masses and lepton flavor violating (LFV) processes. These symmetries are, however, not respected by higher-dimensional operators beyond the SM suppressed by some new physics scale  $\Lambda$ . In fact, already at the first order in the  $1/\Lambda$  expansion (dimension-five operators), we find that lepton number can be broken in two units,  $\Delta L_i = 2$ , generating then neutrino masses. The smallness of the neutrino masses however forces the scale suppressing these operators  $\Lambda$  to be extremely large (or the corresponding Wilson coefficients extremely small), making the physical effects of these operators only visible in neutrino physics.

We are here interested in LFV processes where the relative lepton numbers are violated, but the total lepton number is preserved. These processes are among the best indirect probes for new physics at the TeV [1]. This is due to the fact that  $L_{e,\mu,\tau}$  are not easy to arise accidentally in scenarios beyond the SM (BSM), where the matter content and interactions are much more extended than the simple leptonic sector of the SM. As a consequence, sizable BSM effects are expected to arise in LFV processes. They can be characterized by dimension-six operators ( $\sim 1/\Lambda^2$ ) that, as they preserve the total lepton number, do not need to be as highly suppressed as dimension-five operators. For this reason they can have an important impact in future LFV experiments involving the charged lepton sector.

We will consider in particular LFV processes with  $\Delta L_e = \Delta L_\mu = 1$ . At present, the most competitive experimental measurements come from the processes  $\mu \rightarrow e\gamma$ ,  $\mu \rightarrow eee$  and  $\mu N \rightarrow eN$  (see table 1), and these will improve in the near future. Especially, the sensitivities of  $\mu \rightarrow eee$  and  $\mu N \rightarrow eN$  are expected to improve by four orders of magnitude by the mid-2020s [2]. These LFV processes are very clean observables from the theoretical point of view, since the contributions of the SM (even when implemented with neutrino masses) are much smaller than the present and future experimental sensitivities. We will also consider  $h \rightarrow \mu e$ , although, as we will show, it does not place any important constraint. There are other LFV processes such as  $Z \rightarrow \mu e$  and  $J/\psi \rightarrow \mu e$ , but they are not competitive with those in table 1. We also have processes involving flavor violations in the quark sector, e.g.  $K \rightarrow \mu e$ , but these quark flavor transitions are quite constrained from other non LFV processes, so we will not consider them here.

We will use the Effective Field Theory (EFT) approach to characterize the BSM contributions to LFV processes as they are captured in the Wilson coefficients of the dimension-six operators. Our purpose is to understand at what order in the loop expansion the Wilson coefficients can enter into the different observables of table 1. Depending on the experimental sensitivity, we will see that certain Wilson coefficients can be better bounded by  $\mu \rightarrow e\gamma$  even when they enter at the two-loop level.

This program will therefore require the calculation of anomalous dimensions at the two-loop level. We will use on-shell methods to perform these calculations. It has already been shown the efficiency of these methods to calculate anomalous dimensions at the loop level [3–9], where these can be reduced to products of tree-level amplitudes integrated over a phase space. On-shell amplitude methods are also able to show in a transparent way many selection rules hidden in the ordinary Feynman approach [10–17], mainly due to helicity [11] or angular momentum conservation [14, 15]. This simplifies substantially the loop calculations.<sup>1</sup>

Our calculation of the anomalous dimensions at the two-loop level will in particular show how  $\mu \rightarrow e\gamma$  can constrain the LFV couplings  $W\mu\nu_e$  and  $h\mu e$  and some four-fermion interactions at an unprecedented level. Previous (partial) analysis can be found in refs. [22–28].<sup>2</sup>

In section 2 we review the LFV dimension-six operators of the SM EFT and the tree-level bounds derived from the processes in table 1. In section 3 we analyze which operators

<sup>1</sup>On-shell techniques for the SM EFT have also been applied in related contexts [18–21].

<sup>2</sup>For similar studies on LFV processes involving  $\tau$  leptons, see for example refs. [29–32].

	BR( $\mu \rightarrow e\gamma$ )	BR( $\mu \rightarrow eee$ )	$R(\mu N \rightarrow eN)$	BR( $h \rightarrow \mu e$ )
<b>Current</b>	$4.2 \cdot 10^{-13}$ [33]	$1 \cdot 10^{-12}$ [34]	$7 \cdot 10^{-13}$ [35]	$6.1 \cdot 10^{-5}$ [36]
<b>Future</b>	$6.0 \cdot 10^{-14}$ [37]	$1 \cdot 10^{-16}$ [38]	$8 \cdot 10^{-17}$ [39]	

**Table 1.** Current and near future upper bounds on  $\Delta L_e = \Delta L_\mu = 1$  processes.

mix into the dipole operators responsible for  $\mu \rightarrow e\gamma$ . We find that there are various important two-loop anomalous dimension matrix elements that are unknown. Section 4 is then dedicated to compute these missing pieces of the two-loop renormalization group (RG) equation, via on-shell methods. In sections 5 and 6 we analyze the RG mixing of dimension-six operators into the  $\mu \rightarrow eee$  and  $\mu N \rightarrow eN$  processes, respectively. A global perspective of the new loop effects we have found from mixings into the LFV observables is summarized in section 7. For illustration, in section 8 we show the impact of our analysis on two simple UV completions of the SM EFT. Finally, we conclude in section 9.

## 2 LFV dimension-six operator basis

The relevant dimension-six operators for our analysis of processes with  $\Delta L_e = \Delta L_\mu = 1$  are given by

$$\mathcal{L}_6 = C_{DW}^{\mu e} \frac{y_\mu g}{\Lambda^2} \bar{L}_L^{(2)} \tau^a \sigma^{\mu\nu} e_R^{(1)} H W_{\mu\nu}^a + C_{DB}^{\mu e} \frac{y_\mu g'}{\Lambda^2} \bar{L}_L^{(2)} \sigma^{\mu\nu} e_R^{(1)} H B_{\mu\nu} + (\mu \leftrightarrow e) \quad (2.1)$$

$$+ \frac{C_{L3}^{\mu e}}{\Lambda^2} (H^\dagger i \overleftrightarrow{D}_\mu H) (\bar{L}_L^{(2)} \gamma^\mu L_L^{(1)}) + \frac{C_{L3}^{\mu e}}{\Lambda^2} (H^\dagger i \overleftrightarrow{D}_\mu H) (\bar{L}_L^{(2)} \tau^a \gamma^\mu L_L^{(1)}) + \frac{C_{R3}^{\mu e}}{\Lambda^2} (H^\dagger i \overleftrightarrow{D}_\mu H) (\bar{e}_R^{(2)} \gamma^\mu e_R^{(1)}) \quad (2.2)$$

$$+ C_y^{\mu e} \frac{y_\mu}{\Lambda^2} (H^\dagger H) (\bar{L}_L^{(2)} e_R^{(1)} H) + (\mu \leftrightarrow e) \quad (2.3)$$

$$+ \frac{C_{LL}^{\mu e ff}}{\Lambda^2} (\bar{L}_L^{(2)} \gamma_\mu L_L^{(1)}) (\bar{F}_L \gamma^\mu F_L) + \frac{C_{LL3}^{\mu e ff}}{\Lambda^2} (\bar{L}_L^{(2)} \tau^a \gamma_\mu L_L^{(1)}) (\bar{F}_L \tau^a \gamma^\mu F_L) + \frac{C_{RR}^{\mu e ff}}{\Lambda^2} (\bar{e}_R^{(2)} \gamma_\mu e_R^{(1)}) (\bar{f}_R \gamma^\mu f_R)$$

$$+ \frac{C_{LR}^{\mu e ff}}{\Lambda^2} (\bar{L}_L^{(2)} \gamma_\mu L_L^{(1)}) (\bar{f}_R \gamma^\mu f_R) + \frac{C_{RL}^{\mu e ff}}{\Lambda^2} (\bar{e}_R^{(2)} \gamma^\mu e_R^{(1)}) (\bar{F}_L \gamma_\mu F_L)$$

$$+ C_{LR}^{\mu lle} \frac{y_\mu}{\Lambda^2} (\bar{L}_L^{(2)} \gamma_\mu L_L) (\bar{e}_R \gamma^\mu e_R^{(1)}) + C_{LR}^{\mu qqe} \frac{y_\mu}{\Lambda^2} (\bar{L}_L^{(2)} \gamma_\mu Q_L) (\bar{d}_R \gamma^\mu e_R^{(1)}) + (\mu \leftrightarrow e) \quad (2.4)$$

$$+ C_{LuQe}^{\mu eqq} \frac{y_\mu}{\Lambda^2} (\bar{L}_L^{(2)} u_R) (\bar{Q}_L e_R^{(1)}) + C_{LeQu}^{\mu eqq} \frac{y_\mu}{\Lambda^2} (\bar{L}_L^{(2)} e_R^{(1)}) (\bar{Q}_L u_R) + (\mu \leftrightarrow e) + \text{h.c.}, \quad (2.5)$$

where  $y_\mu = \sqrt{2} m_\mu / v$  ( $v = 246$  GeV) is the SM muon Yukawa coupling and  $g, g'$  are the  $SU(2)_L$  and  $U(1)_Y$  couplings as defined in appendix B. We also have  $F_L = Q_L, L_L$  and  $f_R = u_R, d_R, e_R$  the SM left-handed  $SU(2)_L$  doublets and right-handed  $SU(2)_L$  singlets respectively. We only specify the flavor indices for the  $\mu e$  transitions where the superindices 1, 2 corresponds to  $e, \mu$ . We also have factored out a  $y_\mu$  in operators involving  $\bar{L}_L^{(2)} e_R^{(1)}$  or  $L_L^{(1)} e_R^{(2)}$  where the  $\mu e$  transitions have a change of chirality. Therefore, in the interchange  $\mu \leftrightarrow e$  in  $\mathcal{L}_6$  we keep fixed  $y_\mu$ .

The four-fermion operators have been separated into two groups: eq. (2.4) are operators of type  $\psi^2 \bar{\psi}^2$  in Weyl notation, while eq. (2.5) are operators of type  $\psi^4$  (and  $\bar{\psi}^4$ ). They have respectively total helicity  $h = 0$  and  $h = \pm 2$ . This is important as we will see later for

understanding the renormalization mixing. As compared to the Warsaw basis [40], we have made the replacement<sup>3</sup>

$$\mathcal{O}_{lequ}^{(3)} = (\bar{L}_L \sigma_{\mu\nu} e_R)(\bar{Q}_L \sigma^{\mu\nu} u_R) \rightarrow \mathcal{O}_{LuQe} = (\bar{L}_L u_R)(\bar{Q}_L e_R), \quad (2.6)$$

and we have written differently the operator (via Fierzing)

$$\mathcal{O}_{ledq} = (\bar{L}_L e_R)(\bar{d}_R Q_L) = -\frac{1}{2}(\bar{L}_L \gamma_\mu Q_L)(\bar{d}_R \gamma^\mu e_R), \quad (2.7)$$

to make it clear that this is an operator of the type  $\psi^2 \bar{\psi}^2$  with total helicity  $h = 0$ .

It will be important for later to understand the impact of the operators (2.2) to write them in the unitary gauge:

$$\begin{aligned} -(v+h)^2 & \left[ \frac{C_L^{\mu e} + C_{L3}^{\mu e}}{\Lambda^2} \left( \frac{g}{2c_{\theta_W}} Z^\mu \bar{\mu}_L \gamma_\mu e_L - \frac{g}{2\sqrt{2}} [W^{+\mu} \bar{\nu}_{\mu L} \gamma_\mu e_L + \text{h.c.}] \right) \right. \\ & + \frac{C_L^{\mu e} - C_{L3}^{\mu e}}{\Lambda^2} \left( \frac{g}{2c_{\theta_W}} Z^\mu \bar{\nu}_{\mu L} \gamma_\mu \nu_{eL} + \frac{g}{2\sqrt{2}} [W^{+\mu} \bar{\nu}_{\mu L} \gamma_\mu e_L + \text{h.c.}] \right) \\ & \left. + \frac{C_R^{\mu e}}{\Lambda^2} \frac{g}{2c_{\theta_W}} Z^\mu \bar{\mu}_R \gamma_\mu e_R \right] + (\mu \leftrightarrow e), \end{aligned} \quad (2.8)$$

which shows that these operators induce a LFV coupling for the  $Z$ ,  $W$  and  $hW, hZ$ . Custodial symmetry together with a  $L \leftrightarrow R$  parity can protect some of these couplings. For example, as explained in ref. [41], these symmetries can impose  $C_L + C_{L3} = 0$  such that the LVF  $Z\mu e$  and  $hZ\mu e$  couplings are zero. Therefore, for BSM sectors respecting these symmetries, the only LFV couplings will involve neutrinos which are difficult to detect, implying that no strong bounds can be derived from direct measurements such as  $W \rightarrow \mu \bar{\nu}_e, e \bar{\nu}_\mu$  or  $Z \rightarrow \nu_\mu \bar{\nu}_e$ . As we will see, loop effects will be important to get better bounds from other LFV observables.

## 2.1 LFV experimental constraints at the tree level

The Wilson coefficients of the operators (2.2)–(2.5) are constrained from the LFV observables of table 1. In this section we want to review the bounds obtained from a tree-level analysis. The result is presented in table 2 in black color (see refs. [22–25] for previous analysis). The aim of this analysis is to understand which loop effects mixing the different Wilson coefficients of (2.2)–(2.5) are important to consider in order to obtain better bounds. These loop calculations and the discussion of how much the bounds are improved will be presented in the next sections.

The current constraint on the dipoles  $C_{DW,DB}^{e\mu,\mu e}$  of eq. (2.1) is dominated by the experimental bound on  $\text{BR}(\mu \rightarrow e\gamma)$  at which they enter at tree level (see eq. (3.3)). This leads to

$$\frac{1}{\Lambda^2} \sqrt{|C_{DW}^{\mu e} - C_{DB}^{\mu e}|^2 + |C_{DW}^{e\mu} - C_{DB}^{e\mu}|^2} \lesssim 1 \cdot 10^{-6} \frac{1}{\text{TeV}^2}, \quad (2.9)$$

<sup>3</sup>Using Fierz identities, we have the relation  $\mathcal{O}_{lequ}^{(3)} = -8\mathcal{O}_{LuQe} - 4\mathcal{O}_{LeQu}$ .

	$\mu \rightarrow e\gamma$	$\mu \rightarrow eee$	$\mu N \rightarrow eN$	$h \rightarrow \mu e$
$C_{DB}^{\mu e} - C_{DW}^{\mu e}$	951 TeV (1547 TeV)	218 TeV (2183 TeV)	208 TeV (1812 TeV)	
$C_{DB}^{\mu e} + C_{DW}^{\mu e}$	127 TeV (214 TeV)	26 TeV (309 TeV)	24 TeV (253 TeV)	
$C_R^{\mu e}$	35 TeV (59 TeV)	160 TeV (1602 TeV)	225 TeV (1535 TeV)	
$C_L^{\mu e} + C_{L3}^{\mu e}$	4 TeV (7 TeV)	164 TeV (1642 TeV)	225 TeV (1535 TeV)	
$C_L^{\mu e} - C_{L3}^{\mu e}$	24 TeV (41 TeV)	35 TeV (421 TeV)	50 TeV (395 TeV)	
$C_{LuQe}^{\mu ett}$	304 TeV (510 TeV)	63 TeV (735 TeV)	59 TeV (604 TeV)	
$C_{LeQu}^{\mu ett}$	80 TeV (141 TeV)	14 TeV (209 TeV)	5 TeV (57 TeV)	
$C_{LL(RR),LR(RL)}^{\mu eee}$		207,174 TeV (2070,1740 TeV)		
$C_{LL,RR,LR}^{\mu euu}$			352 TeV (2693 TeV)	
$C_{LL,RR,LR}^{\mu edd}$			376 TeV (2725 TeV)	
$C_{LR}^{\mu dde}$			18 TeV (164 TeV)	
$C_{LL,RR,LR,RL}^{\mu e\tau\tau}$		14,16,14,16 TeV (174,194,174,194 TeV)	22 TeV (200 TeV)	
$C_{LL3}^{\mu e\tau\tau}$		20 TeV (247 TeV)	55 TeV (476 TeV)	
$C_{LL,RR,LR,RL}^{\mu ett}$	122 TeV (214 TeV)	21 TeV (317 TeV)	22,32,32,22 TeV (200,290,290,200 TeV)	
$C_{LL3}^{\mu ett}$	230 TeV (401 TeV)	41 TeV (592 TeV)	100 TeV (851 TeV)	
$C_{LL,RR,LR,RL}^{\mu ebb}$		14,16,14,16 TeV (174,194,174,194 TeV)	22 TeV (200 TeV)	
$C_y^{\mu e}$	4 TeV (6 TeV)	1 TeV (9 TeV)	1 TeV (7 TeV)	0.3 TeV

**Table 2.** Present (future) lower bounds on  $\Lambda$  of the dimension-six operators (2.2)–(2.5) from the different LFV violating processes. We have fixed the Wilson coefficient  $C_i = 1$ , turning each one by one. We show the bound in black, blue, purple and red depending on whether the Wilson coefficients contribute to the observables at the tree-level, one-loop single-log, two-loop double-log or two-loop single-log order, respectively. Blank spaces correspond to contributions that we estimate to be too small to be competitive with existing bounds.

and will improve by almost an order of magnitude in the future. Eq. (2.9) provides a very strong constraint that shows that renormalization effects to  $(C_{DW} - C_{DB})$  arising from other Wilson coefficients  $C_i$  could also place strong constraints on these latter. These effects can be important even when they arise at the two-loop level, e.g.  $\Delta(C_{DW} - C_{DB}) \sim C_i/(16\pi^2)^2 \sim 10^{-4}$ , where we estimate to obtain  $C_i/\Lambda^2 \lesssim 1/(6 \text{ TeV})^2$ . Therefore an analysis of anomalous dimension mixings into  $C_{DW,DB}$  is needed up to the two-loop level. The Wilson coefficient  $(C_{DW} - C_{DB})$  also enters at tree level in the observables  $\mu \rightarrow 3e$  and  $\mu N \rightarrow eN$  (see eq. (5.1) and eq. (6.2) respectively), but the present constraints are not so competitive, as shown in table 2. Nevertheless, the spectacular prospects of improvement by four orders of magnitude in each of them will lead to an improved bound on  $(C_{DW} - C_{DB})$  that could overcome that from  $\mu \rightarrow e\gamma$ .

Let us consider now the four-fermion interactions (2.4) and (2.5). In particular, the operators of type  $\mu\bar{e}\bar{e}e$  enter at tree level to  $\mu \rightarrow 3e$  and provide the limits

$$\frac{C_{LL,RR}^{\mu e e e}}{\Lambda^2} \lesssim 2.3 \cdot 10^{-5} \frac{1}{\text{TeV}^2}, \quad \frac{C_{LR,RL}^{\mu e e e}}{\Lambda^2} \lesssim 3.3 \cdot 10^{-5} \frac{1}{\text{TeV}^2}. \quad (2.10)$$

They are clearly not as strong as that in (2.9), but in the near future this bound is expected to improve by two orders of magnitude, being then comparable to eq. (2.9). Therefore loop effects mixing other Wilson coefficients into  $C_{LL,RR,LR,RL}^{\mu e e e}$  should also be considered. As we will see, however, all the relevant LFV Wilson coefficients enter into the anomalous dimensions of  $C_{LL,RR,LR,RL}^{\mu e e e}$  at the one-loop level, making two-loop effects not necessary. Similar conclusions can be reached for four-fermion interactions of type  $\mu\bar{e}\bar{u}u$  and  $\mu\bar{e}\bar{d}d$  that are constrained by  $\mu N \rightarrow eN$  at a similar level as in eq. (2.10).

The Wilson coefficients of eq. (2.2) give rise to the LFV  $Z\mu e$  coupling (see eq. (2.8)), and therefore can enter at tree level into the observables  $\mu \rightarrow 3e$  and  $\mu N \rightarrow eN$  (see eq. (5.1) and eq. (6.2) respectively), providing a bound similar to (2.10). There are also direct bounds from  $Z \rightarrow \mu e$  but these are not so competitive (one gets constraints of order  $\Lambda \gtrsim 5 \text{ TeV}$ ). It is important to remark again that the induced  $Z\mu e$  coupling is proportional to the combination  $(C_L^{\mu e} + C_{L3}^{\mu e})$ , and therefore tree-level constraints from  $\mu \rightarrow 3e$  and  $\mu N \rightarrow eN$  are only on this specific combination. As we already discussed, the orthogonal combination  $(C_L^{\mu e} - C_{L3}^{\mu e})$  only enters at tree level into LFV gauge boson couplings involving neutrinos, implying that no relevant bounds on this combination can be placed at this order. Loop effects however can be important as we will discuss in the next section. The parametrization of the bounds using these two particular combinations has also a theoretical motivation, since, as we already mentioned, BSM models can give sizable contributions to  $(C_L^{\mu e} - C_{L3}^{\mu e})$  but not to  $(C_L^{\mu e} + C_{L3}^{\mu e})$  as this latter is protected by a custodial symmetry [41]. We provide an example in section 8.1.

The last operator to consider is (2.3) that can only enter at tree level in Higgs physics, specifically in  $h \rightarrow \mu e$ .<sup>4</sup> The bound (see table 2) is very weak, therefore it is expected that bounds from other observables, where  $C_y^{\mu e, e\mu}$  can enter via mixing at the loop level, can be potentially stronger. We will indeed see that this operator enters at the two-loop level into  $\mu \rightarrow e\gamma$  and gets a much more severe constraint.

---

<sup>4</sup>These Wilson coefficients enter as  $\text{BR}(h \rightarrow \mu e) = m_H m_\mu^2 v^2 [|C_y^{\mu e}|^2 + |C_y^{e\mu}|^2]/(8\pi\Gamma_H\Lambda^4)$ .

We conclude that there are some Wilson coefficients whose loop effects can be potentially relevant for the observables  $\mu \rightarrow e\gamma$ ,  $\mu \rightarrow 3e$  and  $\mu N \rightarrow eN$ . Below we will calculate the anomalous dimensions at the two-loop level for these  $C_i$  that will allow us to obtain new competitive bounds.

### 3 $\mu \rightarrow e\gamma$ in the SM EFT

The  $\mu \rightarrow e\gamma$  process arises from the Lagrangian term

$$-\frac{4G_F}{\sqrt{2}} m_\mu [d_{\mu e} \bar{\mu}_L \sigma^{\mu\nu} e_R F_{\mu\nu} + d_{e\mu} \bar{e}_L \sigma^{\mu\nu} \mu_R F_{\mu\nu} + \text{h.c.}], \quad (3.1)$$

where  $d_{\mu e, e\mu}$  must be evaluated at the muon mass scale. The branching ratio is given by [42]

$$\text{BR}(\mu \rightarrow e\gamma) = 384\pi^2 (|d_{\mu e}|^2 + |d_{e\mu}|^2), \quad (3.2)$$

where the large factor is because the LFV decay is a two-body process, while the dominating muon decay channel is a three-body one. This decay process is tightly constrained and further sensitivity is expected in the near future, see table 1.

At tree level the only Wilson coefficients of the SM EFT that enter into  $d_{\mu e}$  are the dipoles  $C_{DW, DB}^{\mu e}$ :

$$d_{\mu e} = \frac{e v^2}{2\Lambda^2} (C_{DW}^{\mu e} - C_{DB}^{\mu e}), \quad (3.3)$$

where  $e = g \sin \theta_W$ , and similarly for  $d_{e\mu}$  by exchanging  $\mu \leftrightarrow e$ .

We are interested in operator mixing into the dipoles (3.1). There are various effects to be considered: (i) finite matching contributions from a new physics scale  $\Lambda$ , (ii) RG mixing from  $\Lambda$  to the electroweak scale  $m_W$ , (iii) finite threshold corrections arising from integrating out the  $W$ ,  $Z$ , Higgs and the heavy SM fermions, and (iv) RG mixing from the electroweak scale  $m_W$  to  $m_\mu$ . At the leading order (one-loop level) the UV matching threshold (i) and SM IR matching (iii) lead to finite contributions to the dipoles. These type of corrections are model dependent, and can (partially) cancel against each other as they involve rational coefficients, apart from some overall couplings. We will show examples in which this occurs in section 8.1. Here we are instead interested in contributions from RG running, which correct the tree-level dipoles by logarithms  $\ln(\Lambda/m_W)$ , raised to a suitable power, which are hardly possible to cancel against matching contributions of either type (i) and (iii). In particular we are interested in the leading RG mixings from any operator, other than the dipoles, into the dipoles. Our aim is to understand to which physics a precise measurement of (3.2) is sensitive. Therefore, we will only keep track of the leading RG mixing contribution from any dimension-six operator into (3.1).

At the one-loop level, selection rules, mainly based on spurious SUSY [10] or helicity arguments [11], dictate the anomalous dimension mixing terms  $\mathcal{O}_i \rightarrow \mathcal{O}_j$ . Of particular importance is the selection rule  $\Delta n \geq |\Delta h|$  [11], where  $\Delta n = n_f - n_i$  and  $\Delta h = h_f - h_i$ , being  $n$  ( $h$ ) the number of fields (helicity) of the operator. There is only one exception to this rule,  $\bar{\psi}^2 \psi^2 \leftrightarrow \psi^4$  only when the loop involves the Yukawa product  $y_u y_d$  or  $y_u y_e$ . In the particular case of dipole operators that have  $n = 4, |h| = 2$ , the only operators that can



mix into them are those with helicity  $|h| = 2$ . This reduces to the four-fermion operators in (2.5), apart from the orthogonal combination  $(C_{DW}^{\mu e} + C_{DB}^{\mu e})$ . The one-loop RG mixing from  $\mathcal{O}_{LeQu}^{\mu e q q}$  however is trivially absent because  $\bar{L}^{(2)}e^{(1)}$  is external to the loop calculation and does not have the dipole structure (and similarly for  $\mathcal{O}_{LeQu}^{e \mu q q}$ ). This argument leaves out only the following possibility for one-loop leading-log contributions:

$$C_{LuQe} \longrightarrow C_{DW,DB}, \tag{3.4}$$

where we suppressed flavor indices. The calculation of the one-loop RG mixing in (3.4) was done in [43] and recently revisited in [5] with on-shell methods. The result is presented in section 4.1.

At the two-loop level, there are other various dimension-six operators that can mix with the dipoles. We can classify them according to a logarithmic expansion. At leading order we have two-loop double-log contributions proportional to

$$\frac{C_i C_j}{(16\pi^2)^2} \ln^2(\Lambda/m_W), \quad i \neq j. \tag{3.5}$$

These contributions arise from mixings of the type  $\mathcal{O}_i \xrightarrow{1\text{-loop}} \mathcal{O}_j \xrightarrow{1\text{-loop}} \mathcal{O}_{DW,DB}$ . Again, selection rules [10, 11] only allow operator mixing between those with equal  $h$ , in particular,  $\mathcal{O}_{LeQu} \rightarrow \mathcal{O}_{LuQe} \rightarrow \mathcal{O}_{DW,DB}$ , with the exception of  $\bar{\psi}^2 \psi^2 \rightarrow \psi^4 \rightarrow \psi^2 \phi F$  where the first step can occur if it involves the product of Yukawa couplings  $y_u y_d$  or  $y_u y_e$ . There are double logs of the type  $C_i^2 \ln^2(\Lambda/m_W)/(16\pi^2)^2$  as well. However these are sub-leading corrections to already existing one-loop effects. The second type of corrections are two-loop single-log contributions

$$\frac{C_i}{(16\pi^2)^2} \ln(\Lambda/m_W). \tag{3.6}$$

There are only three of such two-loop mixings:  $\psi^2 \phi^3, \psi^2 \bar{\psi}^2 \rightarrow \psi \phi F$ , which were computed in [4, 44], and  $\bar{\psi} \gamma \psi H^\dagger D H \rightarrow F_{\mu\nu} \bar{\psi} H \psi$ , which will be calculated here for the first time.

We summarize the structure of the one- and two-loop mixing pattern into dipoles in figure 1. In the next section we present the calculation of the relevant anomalous dimensions of dipole Wilson coefficients up to the two-loop level. Our task is greatly simplified by using on-shell methods as we explain next.

## 4 The on-shell way

Let us start presenting the basic concepts necessary for the computation of anomalous dimensions from on-shell amplitudes. Our calculations are based on the formula [3]

$$\langle \vec{n} | \mathcal{O}_j | 0 \rangle^{(0)} \gamma_{ji}^{(1)} = -\frac{1}{\pi} \langle \vec{n} | \mathcal{M} \otimes \mathcal{O}_i | 0 \rangle^{(0)}, \tag{4.1}$$

which allows to compute the leading correction to the anomalous dimension matrix  $\gamma_{ji}^{(1)}$  with  $i \neq j$ . On the left-hand side (l.h.s.) of (4.1) we have a form factor computed in the

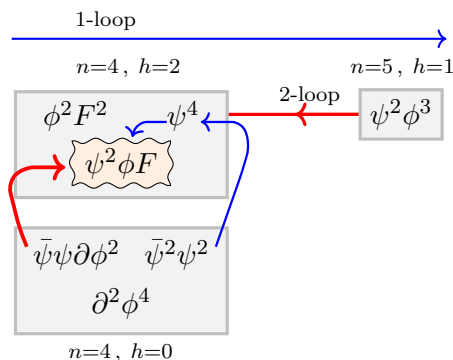


**Figure 1.** Structure of the RG mixings from dimension-six operators into LFV dipoles. One-loop RG mixing can only proceed from left to right, generating mixing between operators belonging to different helicity boxes (shown in grey), and within operators belonging to the same helicity box. One-loop mixing from the category  $(n, h) = (4, 0)$  into  $(4, 2)$  is forbidden by spurious SUSY [10] or helicity [11] selection rules, except for the non-holomorphic contribution proportional to  $y_u y_d$  or  $y_u y_e$ , which mixes the  $\psi^4$  and  $\bar{\psi}^2 \psi^2$  four-fermion operators at one loop. In blue and red we indicate the relevant RG mixings for the LFV dipoles at one- and two-loop precision, respectively.

free theory, i.e. at zero order in the coupling, denoted as minimal form factor. For instance, the minimal form factors of the dipoles are given by

$$\langle 1_{L_l}^- 2_B^- 3_e^- 4_{H_k} | \mathcal{O}_{DB} | 0 \rangle^{(0)} = 2\sqrt{2} g' y_\mu \langle 12 \rangle \langle 23 \rangle \epsilon_{lk}, \quad (4.2)$$

$$\langle 1_{L_l}^- 2_{W\alpha}^- 3_e^- 4_{H_k} | \mathcal{O}_{DW} | 0 \rangle^{(0)} = 2\sqrt{2} g y_\mu \langle 12 \rangle \langle 23 \rangle \epsilon_{lk'} (\tau^\alpha)_k^{k'}, \quad (4.3)$$

where  $\epsilon$  and  $\tau$  are tensors of  $SU(2)_L$ .<sup>5</sup> The form factors  $\langle \vec{n} | \mathcal{O}_j | 0 \rangle^{(0)}$  are polynomials of the kinematical variables  $\{|i\rangle, |i']\}$ , i.e. the spinor-helicity variables.<sup>6</sup> On the right-hand side (r.h.s.), the symbol ‘ $\otimes$ ’ denotes a *dLIPS* phase-space integration over the intermediate states  $\sum_{\vec{m}} |\vec{m}\rangle \langle \vec{m}|$  connecting the on-shell scattering amplitude  $\mathcal{M}(\vec{n} \leftarrow \vec{m})$  and the on-shell form factor  $\langle \vec{m} | \mathcal{O}_i | 0 \rangle$ . The integral over the phase space is often referred to as *unitarity cut*, or *cut* for short. When evaluating the r.h.s. with Feynman diagrams, a cut corresponds to putting on shell the internal propagators crossing the cut, which has the net effect of cutting the Feynman diagram into lower-point diagrams sewed together through the phase-space integral. The upper script (0) means that the r.h.s. of (4.1) is computed to leading non-trivial order so that the unitarity cut  $\langle \vec{n} | \mathcal{M} \otimes \mathcal{O}_i | 0 \rangle^{(0)}$  leads to a polynomial in the kinematical variables, matching the left-hand side of (4.1). Further details and examples can be found in [3, 4, 7].

#### 4.1 One-loop mixing into LFV dipoles

When only two particles cross the cut in the r.h.s. of (4.1), and when only four particles are involved in either the form factor or the amplitude, we are left with the following

<sup>5</sup>Further details on notation are given in appendix B.

<sup>6</sup>Form factors are defined by  $F_{\mathcal{O}}(1 \cdots n; q) = \int d^d x \langle 1 \cdots n | \mathcal{O}(x) | 0 \rangle e^{iqx}$ , where  $\mathcal{O}(x)$  is a local operator and  $\langle 1 \cdots n |$  is an “out” (outgoing) state. In the examples considered in this paper we can smoothly send  $q \rightarrow 0$ . In this limit the form factor is equivalent to a scattering amplitude with an insertion of the EFT operator  $\int d^d x \mathcal{O}(x)$  and with all particles outgoing.

phase-space integral [3]

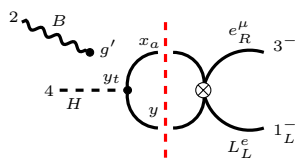
$$\text{Diagram} = -\frac{1}{8\pi^2} \int d\Omega_2 M(12; xy) F_{\mathcal{O}_i}(xy34), \quad (4.4)$$

where the amplitude  $M$  describes the  $x + y \rightarrow 1 + 2$  scattering process, and as usual we have extracted a total delta function  $\langle 12 | \mathcal{M} | xy \rangle = (2\pi)^4 \delta^{(4)}(p_1 + p_2 - p_x - p_y) M(12; xy)$ . The particles of the form factor  $F_{\mathcal{O}_i}(12 \cdots n) \equiv \langle 12 \cdots n | \mathcal{O}_i | 0 \rangle$  are all outgoing. The integral can be easily performed if we write the spinors in the integrand in a basis spanned by two of the external spinors

$$\begin{pmatrix} |x\rangle \\ |y\rangle \end{pmatrix} = \begin{pmatrix} \cos \theta & -e^{i\phi} \sin \theta \\ e^{-i\phi} \sin \theta & \cos \theta \end{pmatrix} \begin{pmatrix} |1\rangle \\ |2\rangle \end{pmatrix}, \quad (4.5)$$

with the measure given by  $d\Omega_2 \equiv \frac{d\phi}{2\pi} 2 \cos \theta \sin \theta d\theta$ . The rotation of  $|x\rangle, |y\rangle$  into  $|1\rangle, |2\rangle$  is obtained by complex-conjugation of (4.5). When identical particles cross the cut in (4.4), one should include an extra combinatorial symmetry factor of  $1/2!$  in the phase space.

As we already explained in the previous section, at the one-loop level we only have eq. (3.4). This computation was done in [5] using unitarity cuts, agreeing with [43, 44]. As a warm-up, we review next such computation. For the case at hand, eq. (4.4) is given by



$$\text{Diagram} \quad (4.6)$$

where on the l.h.s. the gauge boson must be attached in all possible ways to the Higgs (dashed line) or the fermion lines (solid). This results in a two-to-two amplitude given by

$$M(24_k; x_a y) = -\sqrt{2} y_t \left( Y_{t_R} \frac{[xy]^2}{[x2][y2]} + Y_H \frac{[xy][4x]}{[42][x2]} \right) \mathcal{T}_k^a, \quad (4.7)$$

where  $\mathcal{T}_k^a = g' \delta_k^a$  is the  $SU(2)_L$  tensor arising from the contraction of left-handed doublets. On the right-hand side we have the form factor given by

$$F_{\mathcal{O}_{LuQe}^{e\mu tt}}(x_a y 1_l 3) = -y_\mu \langle 1y \rangle \langle x3 \rangle \epsilon_{la}. \quad (4.8)$$

It is now a straightforward matter to plug (4.7) and (4.8) into (4.4), perform the spinor rotations (4.5) and a few elementary integrals, leading to

$$\underbrace{2\sqrt{2} g' y_\mu \langle 12 \rangle \langle 23 \rangle \epsilon_{lk}}_{\text{dipole}} (-y_t) \frac{N_c/2}{(16\pi^2)} (Y_H - 2Y_{t_R}), \quad (4.9)$$

where  $N_c = 3$  is the number of colors and  $y_t$  the top Yukawa coupling. We recognize the minimal form factor of the dipole (4.2) and therefore the anomalous dimension is  $\gamma_{DB} = \frac{y_t}{2} \frac{N_c}{16\pi^2} (Y_{Q_L} + Y_{t_R})$ .

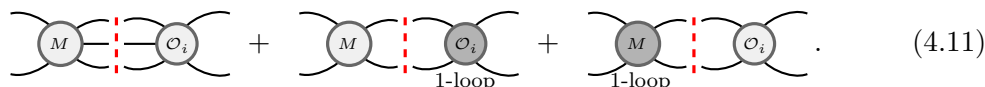
In the case of mixing into  $\mathcal{O}_{DW}$ , we set hypercharges  $Y_{t_R} = 0$  and  $Y_H = 1$  and change the  $SU(2)_L$  tensor to be  $\mathcal{T}_k^a = g(\tau^\alpha/2)_k^a$  on the amplitude side. Then we get the following result:

$$\underbrace{2\sqrt{2}gy_\mu\langle 12\rangle\langle 23\rangle\epsilon_{lk'}(\tau^\alpha)_k^{k'}}_{\text{dipole}}(-y_t)\frac{N_c/4}{(16\pi^2)}. \tag{4.10}$$

From the last expression we recognize the dipole (4.3) and the corresponding anomalous dimension.

### 4.2 Two-loop mixing into dipoles

We want to calculate here the two-loop mixing  $\bar{\psi}\gamma\psi H^\dagger DH \rightarrow F_{\mu\nu}\bar{\psi}H\psi$ , which is the only one relevant for  $\mu \rightarrow e\gamma$  not yet calculated. The two-loop leading-log contributions to the r.h.s. can in principle involve three-particle cuts or two-particle cuts:



$$\text{Diagram 1} + \text{Diagram 2} + \text{Diagram 3}. \tag{4.11}$$

The first diagram involves a tree-level amplitude and a tree-level form factor, so that the three-particle cut accounts for the two-loop factor. The second/third diagram involves a tree-level/one-loop amplitude and a one-loop/tree-level form factor which, together with the two-particle cut, make it to two-loop order. Bellow we will show that the second and third diagrams do not contribute to the  $\bar{\psi}\gamma\psi H^\dagger DH \rightarrow F_{\mu\nu}\bar{\psi}H\psi$  mixings because of simple helicity selection rules. Thus, all our non-trivial calculations will only involve three-particle cuts. For the transition  $\bar{\psi}\gamma\psi H^\dagger DH \rightarrow F_{\mu\nu}\bar{\psi}H\psi$ , in (4.11) we only need to consider two external particles to the scattering amplitude and form factor.

The phase-space integral involving the three-particle cuts can be nicely simplified into the following angular integration [3]

$$\text{Diagram 1} = \frac{\langle 12\rangle[12]}{(16\pi^2)^2} \int d\Omega_3 M(12;xyz) F_{\mathcal{O}_i}(xyz34), \tag{4.12}$$

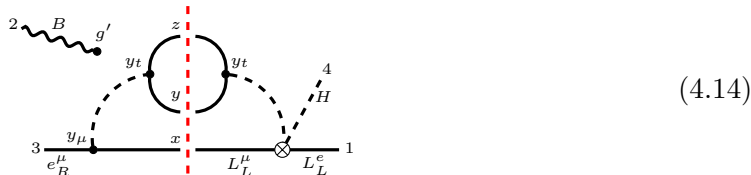
where the amplitude describes the  $x + y + z \rightarrow 1 + 2$  scattering process at tree level. The spinors in the integrand can be rotated in terms of a basis spanned by the two external spinors:

$$\begin{pmatrix} |x\rangle \\ |y\rangle \\ |z\rangle \end{pmatrix} = \begin{pmatrix} \cos\theta_1 & -e^{i\phi}\cos\theta_3\sin\theta_1 \\ \cos\theta_2\sin\theta_1 & e^{i\phi}\left(\cos\theta_1\cos\theta_2\cos\theta_3 - e^{i\delta}\sin\theta_2\sin\theta_3\right) \\ \sin\theta_1\sin\theta_2 & e^{i\phi}\left(\cos\theta_1\cos\theta_3\sin\theta_2 + e^{i\delta}\cos\theta_2\sin\theta_3\right) \end{pmatrix} \begin{pmatrix} |1\rangle \\ |2\rangle \end{pmatrix}, \tag{4.13}$$

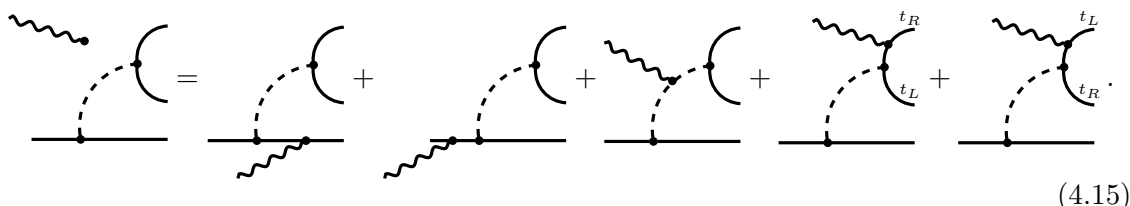
and the measure is  $d\Omega_3 = 4\cos\theta_1\sin^3\theta_1 d\theta_1 2\cos\theta_2\sin\theta_2 d\theta_2 2\cos\theta_3\sin\theta_3 d\theta_3 \frac{d\delta}{2\pi} \frac{d\phi}{2\pi}$ . In the case that  $n$  identical particles cross the cut, one should account for an extra symmetry factor of  $1/n!$  in the phase-space integral, as we will see in some examples in the next sections. Note also that (4.12) includes the  $-1/\pi$  factor in the r.h.s. of (4.1).

### 4.2.1 Top Yukawa $y_t^2$ contributions

We expect this type of contributions to be the dominant ones because they are proportional to  $N_c y_t^2$ . We first explain in detail the mixing of  $\mathcal{O}_L^{e\mu}$  into  $\mathcal{O}_{DB}^{e\mu}$  through a top loop. The three-particle cut is given by



The disconnected gauge boson notation means that the gauge boson must be attached anywhere in the left-hand side of the cut, i.e.



Summing over all such possible attachments of the gauge boson leads to the following tree-level scattering amplitude

$$M_1(32; x_a y_b z) = \sqrt{2} y_t y_\mu \left( Y_{\mu_R} \frac{\langle yz \rangle}{[x2][32]} - Y_{t_R} \frac{\langle x3 \rangle}{[y2][z2]} - Y_H \frac{\langle z3 \rangle}{[y2][x2]} \right) \mathcal{A}_{ba}, \quad (4.16)$$

where  $\mathcal{A}_{ba} = g' \epsilon_{ba}$  is a  $SU(2)_L$  tensor arising from the contraction of the left-handed doublets. We have computed this amplitude using BCFW recursion relation [45, 46] with a Risager shift [47].<sup>7</sup> In (4.16) we have eliminated the hypercharge of the left handed fermions in favour of the Higgs hypercharge and right handed fermions hypercharge. The hypercharges are given by  $(Y_{\mu_R}, Y_{t_R}, Y_H) = (-1, 2/3, 1/2)$ .<sup>8</sup> The tree-level form factor on the r.h.s. of the cut is given by

$$F_{\mathcal{O}_L^{e\mu}}(x_a y_b z 1_l 4_k) = -2 y_t \frac{\langle 14 \rangle [4x]}{\langle yz \rangle} \mathcal{B}_{kl}^{ba}, \quad (4.17)$$

where the  $SU(2)$  tensor is  $\mathcal{B}_{kl}^{ba} = -\delta_k^b \delta_l^a$ . Next we plug (4.16) and (4.17) into (4.12), perform the rotations (4.13),<sup>9</sup> and after some simple algebra and elementary integrations we are led to

$$\underbrace{2\sqrt{2} y_\mu g' \langle 12 \rangle \langle 23 \rangle \epsilon_{lk}}_{\text{dipole}} \frac{-N_c y_t^2}{(16\pi^2)^2} (Y_{\mu_R} + 2Y_H). \quad (4.18)$$

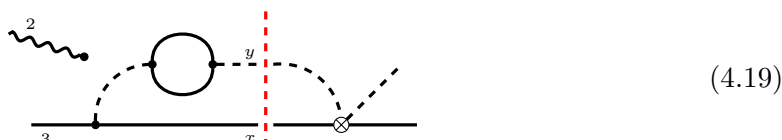
We recognize the minimal form factor of the dipole (4.2).

<sup>7</sup>We emphasise that in (4.16) the particles are not outgoing, instead (4.16) describes the actual physical process  $x_a y_b z \rightarrow 32$ . For crossing fermions we used the same rules as in [3], which can be derived by gluing factorized amplitudes that exchange a fermion, see also appendix of [5].

<sup>8</sup>The hypercharge of the left-handed fermions has been expressed in terms of those of the right-handed fermions and the Higgs  $Y_{\psi_R} + Y_{\psi_L} + Y_H = 0$ .

<sup>9</sup>Note that for the choice of momenta assignments in (4.14) the  $\langle 12 \rangle [12]$  factor in (4.12) should now be  $\langle 32 \rangle [32]$ .

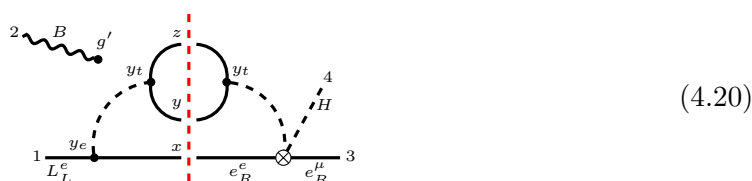
Regarding the two-particle cuts, we will next argue that the second and third diagrams of (4.11) vanish. For the sake of this argument, we will now consider all the particles of the amplitude in the r.h.s. of the cut as outgoing. Eq. (4.4) involves a physical  $\{in\} \rightarrow \{out\}$  amplitude, but as customary in the scattering amplitudes literature, we will cross all particles of the amplitude to be outgoing. Consider first the second diagram of (4.11): the only potential contribution to such cut involves a tree-level amplitude with all negative helicity (outgoing) particles, which vanishes in the SM because such maximal helicity violating amplitude does not exist. Next we consider the third diagram in (4.11), which for our case is



To obtain the l.h.s. scattering amplitude, one must sum over all the diagrams with the gauge boson attached anywhere on the particles to the left of the cut. If the gauge boson is attached to the lepton fermion line, the internal Higgs line goes on shell and the diagram factorizes into a one-loop dressing of the Higgs line and an all negative helicity tree-level diagram that vanishes. If the gauge boson is attached elsewhere (i.e. Higgs lines or top loop), the sum of the diagrams is equal to  $\langle 3x \rangle f(2, y)$ , with  $f$  a function that depends only on the 2 and  $y$  spinors. This amplitude vanishes because it is not possible to build an invariant with  $\langle 2y \rangle$  and  $[2y]$  which has zero helicity for the scalar (of momenta  $p_y$ ) and helicity  $h = -1$  for the gauge boson (of momenta  $p_2$ ).

Therefore the contribution of  $\mathcal{O}_L^{e\mu}$  to  $\mathcal{O}_{DB}^{e\mu}$  proportional to  $N_c y_t^2$  comes only from the three-particle cut (4.14) and is given by  $-N_c y_t^2 (Y_{\mu_R} + 2Y_H) / (16\pi^2)^2$ . This particular contribution is actually zero for the SM hypercharges  $Y_{\mu_R} + 2Y_H = 0$ . This is a surprising accidental zero in the anomalous dimension matrix of the SM EFT operators. However, below we will show that other mixings of the type  $\bar{\psi}\gamma\psi H D H$   $2\text{-loop}$  dipoles are not zero.

The computation of the mixings from  $\mathcal{O}_R^{e\mu}$  to the dipoles is quite analogous: only three-particle cuts matter (for exactly the same reasons as before). The only cut is given by



Again, one must sum over all the diagrams where the gauge boson is attached anywhere on the l.h.s., so that we are led to the following five-point amplitude

$$M_2(1_l 2; x y_b z) = \sqrt{2} y_t y_e \left( -Y_{e_R} \frac{\langle yz \rangle}{[12][x2]} + Y_{t_R} \frac{\langle 1x \rangle}{[y2][z2]} - Y_H \frac{\langle zx \rangle}{[12][y2]} \right) \mathcal{A}_{bl}, \quad (4.21)$$

while the form factor is

$$F_{\mathcal{O}_R^{e\mu}}(x y_b z 3 4_k) = -2 y_t \frac{\langle 34 \rangle [4x]}{\langle yz \rangle} \mathcal{B}_k^b. \quad (4.22)$$

It is again straightforward to perform the rotation (4.13) and integrations in (4.12).<sup>10</sup> The SU(2) tensors  $\mathcal{A}$  and  $\mathcal{B}$  for the  $C_R^{e\mu}$  contributions are given in the table of (4.24) below. We get

$$\underbrace{2\sqrt{2}y_\mu g' \langle 12 \rangle \langle 23 \rangle \epsilon_{lk}}_{\text{dipole}} (Y_{e_R} - Y_H) y_t^2 y_e / y_\mu. \quad (4.23)$$

It is now straightforward to generalize our computation for the remaining mixings from the operators  $\mathcal{O}_L$ ,  $\mathcal{O}_{L3}$  and  $\mathcal{O}_R$  to the dipoles. There are a few minimal changes that we now specify. First, we need to determine the tensors  $\mathcal{A}$  and  $\mathcal{B}$ . We find:

$\mathcal{A} \times \mathcal{B}$	$\mathcal{O}_L$	$\mathcal{O}_{L3}$	$\mathcal{O}_R$
$\mathcal{O}_{DB}$	$g' \epsilon_{ba} \times (-\delta_k^b \delta_l^a)$	$g' \epsilon_{ba} \times (\tau^\beta)_k^b (\tau^\beta)_l^a$	$g' \epsilon_{bl} \times \delta_k^b$
$\mathcal{O}_{DW}$	$g \epsilon_{ba'} (\tau^\alpha / 2)_a^{a'} \times (-\delta_k^b \delta_l^a)$	$g \epsilon_{ba'} (\tau^\alpha / 2)_a^{a'} \times (\tau^\beta)_k^b (\tau^\beta)_l^a$	$g \epsilon_{bl'} (\tau^\alpha / 2)_l^{l'} \times \delta_k^b$

(4.24)

We remark that the  $\mathcal{A}$  and  $\mathcal{B}$  tensors for  $\mathcal{O}_L$  and  $\mathcal{O}_{L3}$  should be used in (4.16) and (4.17), while those of  $\mathcal{O}_R$  are used in (4.21) and (4.22). Next, we note that for the  $\mathcal{O}_{DW}$  computation, apart from using the correct  $\mathcal{A}$  tensors given in (4.24), we also set the hypercharges  $Y_{e_R} = Y_{\mu_R} = Y_{l_R} = 0$ ,  $Y_H = 1$  in the amplitudes (4.16), (4.21), and the SU(2) generators are already included in  $\mathcal{A}$ .

Finally, putting all the contributions together we get the following anomalous dimension matrix  $(\gamma_{C_{DB}^{e\mu}}, \gamma_{C_{DW}^{e\mu}})^T = \gamma_{D1} \cdot (C_L^{e\mu}, C_{L3}^{e\mu}, C_R^{e\mu})^T$  with

$$\gamma_{D1} = \frac{N_c y_t^2}{(16\pi^2)^2} \begin{pmatrix} 0 & 0 & -3y_e/(2y_\mu) \\ 1 & -1 & y_e/(2y_\mu) \end{pmatrix} \approx \frac{N_c y_t^2}{(16\pi^2)^2} \begin{pmatrix} 0 & 0 & 0 \\ 1 & -1 & 0 \end{pmatrix}, \quad (4.25)$$

where in the last step we have neglected the terms of order  $O(y_e/y_\mu) \approx 0$ . The contributions from  $C_L^{\mu e}$ ,  $C_{L3}^{\mu e}$  and  $C_R^{\mu e}$  into the dipoles can be easily obtained by exchanging  $\mu \leftrightarrow e$  in the amplitudes and form factors. We find  $(\gamma_{C_{DB}^{\mu e}}, \gamma_{C_{DW}^{\mu e}})^T = \gamma_{D2} \cdot (C_L^{\mu e}, C_{L3}^{\mu e}, C_R^{\mu e})^T$ , where  $\gamma_{D2}$  is

$$\gamma_{D2} = \frac{N_c y_t^2}{(16\pi^2)^2} \begin{pmatrix} 0 & 0 & -3/2 \\ y_e/y_\mu & -y_e/y_\mu & 1/2 \end{pmatrix} \approx \frac{N_c y_t^2}{(16\pi^2)^2} \begin{pmatrix} 0 & 0 & -3/2 \\ 0 & 0 & 1/2 \end{pmatrix}. \quad (4.26)$$

We note that the contribution of  $\mathcal{O}_L$  and  $\mathcal{O}_{L3}$  to  $\mathcal{O}_{DB}$  is proportional to  $2Y_{e_R} + Y_H = 0$ , which seems to be an accident.

#### 4.2.2 Higgs quartic $\lambda$ contributions

Starting with the mixing from  $\mathcal{O}_L$  to the dipoles, we find two three-particle cuts:

$$\text{Diagram 1} + \text{Diagram 2} \quad (4.27)$$

<sup>10</sup>In this case, given the momenta assignments in (4.20), we have to consider a factor  $\langle 12 \rangle [12]$ .

The amplitude on the first cut (left diagram) is given by

$$M_3(24_k; x_a y_b z_c) = \sqrt{2} \lambda Y_H \left( \frac{[x4]}{[x2][42]} \mathcal{C}_{kc}^{ab} + \frac{[yz]}{[y2][z2]} \mathcal{C}_{ck}^{ba} + \frac{[y4]}{[y2][42]} \mathcal{C}_{kc}^{ba} + \frac{[xz]}{[x2][z2]} \mathcal{C}_{ck}^{ab} \right), \quad (4.28)$$

where the tensors are given by  $\mathcal{C}_{kc}^{ab} = g' \cdot 2\delta_k^a \delta_c^b$ . The form factor is

$$F_{\mathcal{O}_L^{e\mu}}(x_a y_b z_c 1_l 3) = y_\mu \left( \langle 13 \rangle + \frac{2[xz]\langle z1 \rangle}{[3x]} \right) \mathcal{D}_{bla}^c + y_\mu \left( \langle 13 \rangle + \frac{2[yz]\langle z1 \rangle}{[3y]} \right) \mathcal{D}_{alb}^c, \quad (4.29)$$

where  $\mathcal{D}_{bla}^c = (-\delta_b^c \delta_l^a) \epsilon_{l'a}$ . We are introducing these tensors in anticipation of the generalization to non-abelian SU(2) dipoles. It is now straightforward to compute the three-particle cut. We have to compute  $\langle 42 \rangle [42] / ((16\pi^2)^2 2!) \int d\Omega_3 M_3(24_k; x_a y_b z_c) F_{\mathcal{O}_L^{e\mu}}(x_a y_b z_c 1_l 3)$  where note that the symmetry factor 1/2! arises because two identical Higgses cross the cut. After performing the rotations in (4.13) and a few elementary integrals we are led to

$$\text{cut 1} = \frac{12\sqrt{2}\lambda y_\mu g' Y_H \langle 12 \rangle}{(16\pi^2)^2 [32]} s_{24} \left[ 1 + 2\frac{s_{34}}{s_{32}} + 2\frac{s_{34}}{s_{32}} \left( \frac{s_{34} + s_{32}}{s_{32}} \right) \ln \left( \frac{s_{34}}{s_{34} + s_{32}} \right) \right] \epsilon_{lk}, \quad (4.30)$$

where  $s_{ij} = (p_i + p_j)^2$ . Regarding the second cut (right diagram of (4.27)), we need the following amplitude

$$M_4(34_k; x_a y_b z_c) = \lambda y_\mu \frac{1}{[x3]} \mathcal{F}_{akc}^b, \quad (4.31)$$

where  $\mathcal{F}_{akc}^b = 2(\delta_k^b \epsilon_{ac} + \delta_c^b \epsilon_{ak})$ , and the tree-level form factor

$$F_{\mathcal{O}_L^{e\mu}}(x_a y_b z_c 21_l) = 2\sqrt{2} Y_{\mu R} \frac{[xy][xz]\langle yz \rangle}{[12][x2]} \mathcal{G}_{lb}^{ac} + 2\sqrt{2} Y_H \frac{[xy][xz]\langle 1x \rangle}{[y2][z2]} \mathcal{G}_{bl}^{ca}, \quad (4.32)$$

where  $\mathcal{G}_{lb}^{ac} = g'(-\delta_l^a \delta_b^c)$ . Once more, plugging this amplitude and form factor into (4.12) (there is no 1/2! symmetry factor to be included for this cut), performing the rotations and a few simple integrals, we get

$$\text{cut 2} = \frac{12\sqrt{2}\lambda y_\mu g' Y_H \langle 12 \rangle}{(16\pi^2)^2 [32]} s_{34} \left[ 1 - 2\frac{s_{13}}{s_{32}} + 2\frac{s_{13}^2}{s_{32}^2} \ln \left( \frac{s_{13} + s_{32}}{s_{13}} \right) \right] \epsilon_{lk}. \quad (4.33)$$

Each individual cut is non-local, i.e. non-polynomial in the momenta. However, the two-loop contribution to the r.h.s. of (4.1) must be a local contact interaction, because the one-loop mixing  $\mathcal{O}_L \rightarrow \mathcal{O}_{DB}$  is zero. Indeed, after adding the two cuts

$$\text{cut 1} + \text{cut 2} = \underbrace{2\sqrt{2} y_\mu g' \langle 12 \rangle \langle 23 \rangle \epsilon_{lk}}_{\text{dipole}} \frac{6\lambda Y_H}{(16\pi^2)^2}, \quad (4.34)$$

we find that the logs nicely cancel. Therefore the contribution of  $\mathcal{O}_L^{e\mu}$  to  $\mathcal{O}_{DB}^{e\mu}$  proportional to  $\lambda$  is given by  $6\lambda Y_H / (16\pi^2)^2$ .

Next we provide the details of the  $\mathcal{O}_R^{e\mu} \rightarrow \mathcal{O}_{DB}^{e\mu}$  mixing. We need to consider two three-particle cuts:

$$\text{Diagram 1} + \text{Diagram 2} \quad (4.35)$$



The amplitude of the first cut is given by (4.28). The form factor is

$$F_{\mathcal{O}_R^{e\mu}}(x_a y_b z_c 1_l 3) = -y_e \left( \langle 31 \rangle + \frac{2[xz]\langle z3 \rangle}{[1x]} \right) \mathcal{D}_{bla}^c - y_e \left( \langle 31 \rangle + \frac{2[yz]\langle z3 \rangle}{[1y]} \right) \mathcal{D}_{abb}^c, \quad (4.36)$$

where  $\mathcal{D}_{bla}^c = \delta_b^c \delta_l^{l'} \epsilon_{l'a}$ . For the second cut, the amplitude is

$$M_5(1_l 4_k; x y_b z_c) = -\lambda y_e \frac{1}{[1x]} \mathcal{F}_{lkc}^b, \quad (4.37)$$

where  $\mathcal{F}_{lkc}^b = 2(\delta_k^b \epsilon_{lc} + \delta_c^b \epsilon_{lk})$ . Note that there is a sign in (4.37) w.r.t. (4.31) due to crossing; this sign is crucial to get a local result, i.e. that the logs like (4.30) and (4.33) cancel. The form factor is given by

$$F_{\mathcal{O}_R^{e\mu}}(x y_b z_c 3_2) = 2\sqrt{2} Y_{\mu R} \frac{[xz][xy]\langle yz \rangle}{[32][x2]} \mathcal{G}_b^c + 2\sqrt{2} Y_H \frac{[xz][xy]\langle 3x \rangle}{[y2][z2]} \mathcal{G}_b^c, \quad (4.38)$$

where  $\mathcal{G}_b^c = g' \delta_b^c$ . Finally we generalize our computations for the rest of  $\bar{\psi} \gamma \psi H D H \rightarrow$  dipole mixings. It is now a simple matter to do so because the various computations differ only on the  $\mathcal{C} \times \mathcal{D}$  and  $\mathcal{F} \times \mathcal{G}$  tensors, which are given in appendix C. All in all we find that the quartic contribution to  $(\gamma_{C_{DB}^{e\mu}}, \gamma_{C_{DW}^{e\mu}})^T = \gamma_{D3} \cdot (C_L^{e\mu}, C_{L3}^{e\mu}, C_R^{e\mu})^T$  is given by

$$\gamma_{D3} = \frac{\lambda}{(16\pi^2)^2} \begin{pmatrix} 3 & 3 & 3y_e/y_\mu \\ 1 & 3 & y_e/y_\mu \end{pmatrix} \approx \frac{\lambda}{(16\pi^2)^2} \begin{pmatrix} 3 & 3 & 0 \\ 1 & 3 & 0 \end{pmatrix}, \quad (4.39)$$

while the quartic contribution to  $(\gamma_{C_{DB}^{\mu e}}, \gamma_{C_{DW}^{\mu e}})^T = \gamma_{D4} \cdot (C_L^{\mu e}, C_{L3}^{\mu e}, C_R^{\mu e})^T$  is given by

$$\gamma_{D4} = \frac{\lambda}{(16\pi^2)^2} \begin{pmatrix} 3y_e/y_\mu & 3y_e/y_\mu & 3 \\ y_e/y_\mu & 3y_e/y_\mu & 1 \end{pmatrix} \approx \frac{\lambda}{(16\pi^2)^2} \begin{pmatrix} 0 & 0 & 3 \\ 0 & 0 & 1 \end{pmatrix}. \quad (4.40)$$

### 4.3 Finite one-loop contributions at the electroweak scale

Following the EFT approach we have to integrate out the  $W$ ,  $Z$ ,  $h$  and top at the electroweak scale  $\sim m_W$ , and match with the Wilson coefficients of the EFT of photons and light fermions. In this process extra finite contributions to  $d_{\mu e, e\mu}$  may be generated, as can be found in [22]. We are interested in one-loop corrections arising from  $C_{L, L3, R}$  that can compete with our two-loop calculation to the anomalous dimension of  $C_{DW, DB}$ . These are one-loop diagrams involving a  $W$  or a  $Z$  (the Higgs contributions are suppressed by extra Yukawa couplings) in which  $C_{L, L3, R}$  enters via the vertex corrections (2.8). From the  $W$  we get (neglecting terms proportional to  $m_e$ )

$$\Delta d_{e\mu}(m_W) = \frac{e}{32\pi^2} \frac{5}{3} C_{L3}^{e\mu} \frac{v^2}{\Lambda^2}, \quad (4.41)$$

while from the  $Z$  we get

$$\begin{aligned} \Delta d_{e\mu}(m_W) &= -\frac{e}{16\pi^2} \frac{1}{3} (C_L^{e\mu} + C_{L3}^{e\mu}) \left[ \frac{5}{4} - \left( \frac{1}{4} - s_{\theta_W}^2 \right) \right] \frac{v^2}{\Lambda^2}, \\ \Delta d_{\mu e}(m_W) &= +\frac{e}{16\pi^2} \frac{1}{3} C_R^{\mu e} \left[ \frac{5}{4} + \left( \frac{1}{4} - s_{\theta_W}^2 \right) \right] \frac{v^2}{\Lambda^2}. \end{aligned} \quad (4.42)$$

Notice that since  $s_{\theta_W}^2 \approx 1/4$ , these contributions roughly cancel for BSM theories that generate  $C_L^{e\mu} = C_{L3}^{e\mu} \neq 0$ , as occurs in certain models that we will discuss later.

## 5 $\mu \rightarrow eee$ in the SM EFT

The process  $\mu \rightarrow eee$  arises from the Lagrangian terms

$$-\frac{4G_F}{\sqrt{2}} \left[ g_1(\bar{\mu}_R e_L)(\bar{e}_R e_L) + g_2(\bar{\mu}_L e_R)(\bar{e}_L e_R) + g_3(\bar{\mu}_R \gamma_\mu e_R)(\bar{e}_R \gamma_\mu e_R) + g_4(\bar{\mu}_L \gamma^\mu e_L)(\bar{e}_L \gamma_\mu e_L) \right. \\ \left. + g_5(\bar{\mu}_R \gamma^\mu e_R)(\bar{e}_L \gamma_\mu e_L) + g_6(\bar{\mu}_L \gamma^\mu e_L)(\bar{e}_R \gamma_\mu e_R) \right] + \text{h.c.},$$

apart from the dipoles  $d_{\mu e}$  and  $d_{e\mu}$ , that generate the branching ratio [42]

$$\text{BR}(\mu \rightarrow eee) = 2 \left( |g_3|^2 + |g_4|^2 \right) + |g_5|^2 + |g_6|^2 + 32e^2 \left( \ln \left( \frac{m_\mu^2}{m_e^2} \right) - \frac{11}{4} \right) (|d_{\mu e}|^2 + |d_{e\mu}|^2) \\ + 8e \text{Re} \left( d_{e\mu}^* g_6^* + d_{\mu e} g_5^* \right) + 16e \text{Re} \left( d_{e\mu}^* g_4^* + d_{\mu e} g_3^* \right) + \frac{1}{8} \left( |g_1|^2 + |g_2|^2 \right). \quad (5.1)$$

The Wilson coefficients entering into the  $g_i$  at the tree level are

$$g_3 = -\frac{v^2}{2\Lambda^2} \left( C_{RR}^{\mu e e e} + 2s_{\theta_W}^2 C_R^{\mu e} \right), \quad g_4 = -\frac{v^2}{2\Lambda^2} \left( C_{LL}^{\mu e e e} - (1 - 2s_{\theta_W}^2) (C_L^{\mu e} + C_{L3}^{\mu e}) \right), \quad (5.2) \\ g_5 = -\frac{v^2}{2\Lambda^2} \left( C_{RL}^{\mu e e e} - (1 - 2s_{\theta_W}^2) C_R^{\mu e} \right), \quad g_6 = -\frac{v^2}{2\Lambda^2} \left( C_{LR}^{\mu e e e} + 2s_{\theta_W}^2 (C_L^{\mu e} + C_{L3}^{\mu e}) \right),$$

where  $g_{1,2}$  are only induced by dimension-eight operators. Notice that in eq. (5.2) all the Wilson coefficients are associated to operators with  $n = 4$  and  $h = 0$ . Furthermore, we see that  $C_{L,L3}^{\mu e}$  only enter in the combination  $(C_L^{\mu e} + C_{L3}^{\mu e})$ , as they induce  $\mu \rightarrow 3e$  through the  $Z\mu e$  coupling of eq. (2.8).

At the loop level, other Wilson coefficients can mix into the ones in eq. (5.2). In particular, four-fermion  $h = 0$  interactions involving other families or the combination  $(C_L^{\mu e} - C_{L3}^{\mu e})$  can enter into the RGE of the Wilson coefficients of eq. (5.2) at the one-loop level via gauge interactions, as they are also  $n = 4, h = 0$  terms and the mixing is allowed by the  $\Delta n \geq |\Delta h|$  selection rule. The corresponding RGEs are given in the appendix A and the bounds obtained will be discussed later in section 7.

On the other hand,  $C_{LuQe}, C_{LeQu}$ , associated to four-fermion  $|h| = 2$  interactions, and  $C_y^{\mu e}$ , related to an operator with  $n = 5$  and  $|h| = 1$ , cannot mix at the one-loop level with the Wilson coefficients of eq. (5.2), and can only enter into the  $\mu \rightarrow 3e$  observable by mixing into  $d_{\mu e, e\mu}$  as we explained for the  $\mu \rightarrow e\gamma$  case.

## 6 $\mu N \rightarrow eN$ in the SM EFT

The conversion  $\mu \rightarrow e$  in nuclei can arise from the four-fermion terms

$$-\frac{4G_F}{\sqrt{2}} \left[ g_{L,V}^u(\bar{\mu}_L \gamma^\mu e_L)(\bar{u} \gamma_\mu u) + g_{R,V}^u(\bar{\mu}_R \gamma^\mu e_R)(\bar{u} \gamma_\mu u) \right. \\ \left. + g_{L,S}^u(\bar{\mu}_L e_R)(\bar{u} u) + g_{R,S}^u(\bar{\mu}_R e_L)(\bar{u} u) + (u \rightarrow d) \right] + \text{h.c.}, \quad (6.1)$$

defined at the nuclei scale. Also the dipoles  $d_{\mu e}$  and  $d_{e\mu}$  can enter into this observable via the photon splitting into quarks. The branching ratio is given by [48]

$$\text{BR}(\mu \rightarrow e)_N = \frac{2G_F^2}{\omega_{\text{capture}}} \left[ \left| D d_{\mu e} + g_{L,V}^{(p)} V^{(p)} + g_{L,V}^{(n)} V^{(n)} + g_{L,S}^{(p)} S^{(p)} + g_{L,S}^{(n)} S^{(n)} \right|^2 + \left| D d_{e\mu}^* + g_{R,V}^{(p)} V^{(p)} + g_{R,V}^{(n)} V^{(n)} + g_{R,S}^{(p)} S^{(p)} + g_{R,S}^{(n)} S^{(n)} \right|^2 \right], \quad (6.2)$$

where  $\omega_{\text{capture}}$  is the nuclear capture rate of the muon and  $D$ ,  $V^{(p,n)}$ ,  $S^{(p,n)}$  are overlap integrals defined in [48]. We also define

$$\begin{aligned} g_{L/R,V}^{(p)} &= 2g_{L/R,V}^u + g_{L/R,V}^d, & g_{L/R,V}^{(n)} &= g_{L/R,V}^u + 2g_{L/R,V}^d, \\ g_{L/R,S}^{(p)} &= \sum_{q=u,d} G_S^{(q,p)} g_{L/R,S}^q, & g_{L/R,S}^{(n)} &= \sum_{q=u,d} G_S^{(q,n)} g_{L/R,S}^q, \end{aligned} \quad (6.3)$$

with  $G_S^{(u,p)} \simeq G_S^{(d,n)} \simeq 5.1$ ,  $G_S^{(d,p)} \simeq G_S^{(u,n)} \simeq 4.3$ . We have neglected the contribution from the  $s$  quark. At tree level the Wilson coefficients entering into the effective couplings (6.1) are

$$\begin{aligned} g_{L,S}^u &= \frac{v^2}{2\Lambda^2} y_\mu C_{LeQu}^{\mu e u u}, & g_{R,S}^u &= \frac{v^2}{2\Lambda^2} y_\mu C_{LeQu}^{e \mu u u}, & g_{L,S}^d &= \frac{v^2}{\Lambda^2} y_\mu C_{LR}^{\mu d d e}, & g_{R,S}^d &= \frac{v^2}{\Lambda^2} y_\mu C_{LR}^{e d d \mu}, \\ g_{L,V}^u &= -\frac{v^2}{4\Lambda^2} \left[ (C_{LL}^{\mu e u u} + C_{LR}^{\mu e u u}) + 2g_Z^u (C_L^{\mu e} + C_{L3}^{\mu e}) \right], \\ g_{R,V}^u &= -\frac{v^2}{4\Lambda^2} \left[ (C_{RL}^{\mu e u u} + C_{RR}^{\mu e u u}) + 2g_Z^u C_R^{\mu e} \right], \end{aligned} \quad (6.4)$$

and similarly for the down-sector with  $u \rightarrow d$ , where  $g_Z^u = (\frac{1}{2} - \frac{4}{3}s_{\theta_W}^2)$  and  $g_Z^d = (-\frac{1}{2} + \frac{2}{3}s_{\theta_W}^2)$ .

The loop mixing into the Wilson coefficients of eq. (6.4) follows the same pattern as for the  $\mu \rightarrow 3e$  case, as the main difference is the replacement  $ee \rightarrow uu, dd$ . The only new ingredient is the presence of the  $|h| = 2$  operators with Wilson coefficients  $C_{LeQu}^{\mu e u u}$  that can receive one-loop corrections from  $C_{LuQe}^{\mu e u u}$  (and similarly for  $u \rightarrow d$ ). These coefficients however can also receive large corrections at the QCD scale [49] and will not be discussed any further here.

## 7 Constraints from anomalous dimension mixings

In table 2 we present the bounds obtained when anomalous dimension mixing is considered. In blue we show the bounds coming from one-loop mixings into the Wilson coefficients of the observables, while in red are those in which the mixing is at the two-loop level. In purple we show the bounds for those Wilson coefficients entering into the observables by a two-step one-loop mixing, an effect of order (3.5). We remark that we are not including here any finite loop contributions, that could be larger but are also very model dependent as there can be cancellations depending on the details of the model (see next section for particular cases).

Let us start considering the bounds obtained from the two-loop mixings into the dipole transitions  $d_{e\mu, \mu e}$  that is the novel part of this article. The most interesting bound is on the combination  $(C_L^{\mu e} - C_{L3}^{\mu e})$  which, as we explained above, has no serious constraint at

the tree level. Our two-loop calculation of the mixing effect in eq. (4.25) and eq. (4.26) shows that one can get a bound from  $\mu \rightarrow e\gamma$  of order  $\Lambda/\sqrt{C_L^{\mu e} - C_{L3}^{\mu e}} \gtrsim 24$  TeV (assuming a running from that scale). This is quite competitive as compared with bounds coming from a one-loop mixing into  $(C_L^{\mu e} + C_{L3}^{\mu e})$  where this latter is strongly constrained from  $\mu \rightarrow 3e$  and  $\mu N \rightarrow eN$ . The two-loop mixing effect leads to a bound only a factor  $\sim 2$  smaller than that coming from the one-loop mixings. This provides an interesting correlation between these 3 observables, in the sense that if one of them is measured in the near future, the other 2 should also be experimentally accessible. On the other hand, the bound derived on  $(C_L^{\mu e} + C_{L3}^{\mu e})$  from the two-loop mixing into  $\mu \rightarrow e\gamma$  is much weaker (in part, because it is only generated from two loops involving the Higgs, eq. (4.39) and eq. (4.40)) than that from  $\mu \rightarrow 3e$  or  $\mu N \rightarrow eN$  (see table 2). This makes it unfeasible to see this particular BSM effect in  $\mu \rightarrow e\gamma$ .

The other interesting bound from a two-loop mixing into  $\mu \rightarrow e\gamma$  is for  $C_y^{\mu e}$ . One gets  $\Lambda/\sqrt{C_y^{\mu e}} \gtrsim 4$  TeV that clearly overcomes the tree-level bound from  $h \rightarrow \mu e$ . In fact, this result is already telling us that  $\mu \rightarrow e\gamma$  constrains this branching ratio to be  $\text{BR}(h \rightarrow \mu e) \lesssim 2 \cdot 10^{-8}$ , making it inaccessible at the LHC or even at future colliders.<sup>11</sup>

Let us now move to one-loop mixing effects. Although this analysis has been previously done in the literature [1, 22–25], we will provide here an understanding of the quality of the bounds from selection rules of operator mixings [10, 11]. In particular, the only mixing at the one-loop level into the dipoles ( $n = 4, |h| = 2$  operators) is  $C_{LuQe}^{\mu tt}$  whose associated operator has  $n = 4, |h| = 2$ . This operator can be induced from leptoquarks. One gets a quite strong bound,  $\Lambda/\sqrt{C_{LuQe}^{\mu tt}} \gtrsim 304$  TeV. Due to the presence of the Yukawa coupling  $y_t$  in the RGE (see eq. (A.4)) these effects are much smaller for other families. By mixing into this Wilson coefficient  $C_{LuQe}^{\mu tt}$ , other four-fermion operators can enter into  $\mu \rightarrow e\gamma$  by a two step one-loop mixing, and get a bound only slightly weaker (see purple bounds in table 2). In this mixing the  $n = 4, h = 0$  operators need to involve a  $y_t$  Yukawa coupling (as dictated by the only exception to the selection rule  $\Delta n \geq |\Delta h|$  [10, 11]), and as a consequence the mixing is only relevant for Wilson coefficients involving the top.

Finally, other bounds on  $\mu e f f$  operators, where  $f$  can be any SM fermion of the 2nd and 3rd family, can arise by mixing to  $\mu e e e, \mu e u u, \mu e d d$  at the one-loop level. This can occur via gauge interactions as all these operators are  $n = 4, h = 0$ . As seen in table 2 (for the 3rd family, but the same applies for the 2nd), the bounds range between 10–100 TeV, depending on the hypercharges of the states.

## 8 Impact on UV models

As an application of our EFT analysis we would like to consider the impact of the discussed one- and two-loop anomalous dimensions for concrete BSM scenarios. In particular we will consider models with extra heavy fermions and BSM that violate lepton universality.

---

<sup>11</sup>Bounds on  $C_{LR}^{\mu l l e, \mu q q e}$  can also be obtained by a two-loop mixing into  $\mu \rightarrow e\gamma$ , but the contributions are proportional to  $y_{l,d}$ , which leads to weak constraints.

### 8.1 Heavy vector-like fermions

Let us consider a heavy vector-like fermion with mass  $M$  that can either be a singlet ( $S$ ), a hypercharged  $Y_E = -1$  state ( $E$ ), or a  $SU(2)_L$  doublet ( $D$ ). We assume that they couple to the SM by mixing with the SM fermions:

$$\begin{aligned}\Delta\mathcal{L}_S &= (y_S^{(1)}\bar{L}_L^{(1)} + y_S^{(2)}\bar{L}_L^{(2)})S_R i\tau_2 H^* + \text{h.c.}, \\ \Delta\mathcal{L}_E &= (y_E^{(1)}\bar{L}_L^{(1)} + y_E^{(2)}\bar{L}_L^{(2)})E_R H + \text{h.c.}, \\ \Delta\mathcal{L}_D &= (y_D^{*(1)}\bar{e}_R^{(1)} + y_D^{*(2)}\bar{e}_R^{(2)})D_L H^\dagger + \text{h.c.}\end{aligned}\tag{8.1}$$

We would like to calculate their contributions to  $\mu \rightarrow e\gamma$ . Following the EFT approach, we must first integrate out these vector-like states at the scale  $\Lambda = M$  and match these contributions with the Wilson coefficients of (2.2)–(2.5). At tree level, we find

$$\begin{aligned}C_L^{e\mu}(M) &= -C_{L3}^{e\mu}(M) = +\frac{1}{4}y_S^{(1)}y_S^{*(2)}, & \text{for } S, \\ C_L^{e\mu}(M) &= C_{L3}^{e\mu}(M) = -\frac{1}{4}y_E^{(1)}y_E^{*(2)}, & \text{for } E, \\ C_R^{\mu e}(M) &= -\frac{1}{2}y_D^{(1)}y_D^{*(2)}, & \text{for } D,\end{aligned}\tag{8.2}$$

and  $C_{L,R,L3}^{\mu e} = (C_{L,R,L3}^{e\mu})^*$ , as well as

$$\begin{aligned}C_y^{e\mu}(M) &= 0, & C_y^{\mu e}(M) &= 0, & \text{for } S, \\ C_y^{e\mu}(M) &= -y_E^{(1)}y_E^{*(2)}, & C_y^{\mu e}(M) &= -(y_e/y_\mu)y_E^{(2)}y_E^{*(1)} \approx 0, & \text{for } E, \\ C_y^{e\mu}(M) &= -y_D^{(1)}y_D^{*(2)}, & C_y^{\mu e}(M) &= -(y_e/y_\mu)y_D^{(2)}y_D^{*(1)} \approx 0, & \text{for } D,\end{aligned}\tag{8.3}$$

and the Hermitian conjugates  $(C_y)^*$ , which are obtained by complex conjugation of (8.3).

At the one-loop order, these heavy states also contribute to the dipole Wilson coefficients of eq. (3.3). These can be extracted from the contributions to  $(g-2)$  [50]. We find

$$\begin{aligned}C_{DW}^{e\mu}(M) - C_{DB}^{e\mu}(M) &= \frac{1}{6}\frac{y_S^{(1)}y_S^{*(2)}}{16\pi^2}, & \text{for } S, \\ C_{DW}^{e\mu}(M) - C_{DB}^{e\mu}(M) &= \frac{1}{24}\frac{y_E^{(1)}y_E^{*(2)}}{16\pi^2}, & \text{for } E, \\ C_{DW}^{\mu e}(M) - C_{DB}^{\mu e}(M) &= -\frac{1}{24}\frac{y_D^{(1)}y_D^{*(2)}}{16\pi^2}, & \text{for } D.\end{aligned}\tag{8.4}$$

The coefficients  $C_{DW,DB}^{\mu e}$  for  $S, E$ , and  $C_{DW,DB}^{e\mu}$  for  $D$  are both  $O(y_e/y_\mu) \approx 0$ .

Next, we have to evolve these Wilson coefficients from  $M$  to the electroweak scale. In this RG evolution the Wilson coefficients (8.2) and (8.3) mix at the two-loop level with  $C_{DW,DB}^{e\mu,\mu e}$ , in the manner explained in the previous sections. At the electroweak scale, we must now match the theory to the EFT with only photons and light fermions. At the one-loop level, the dipoles can pick up finite terms  $\Delta d_{e\mu}(m_W)$ , which are given by using (4.41)–(4.42) and the tree-level matching coefficients in (8.2). For instance, we

obtain  $\Delta d_{e\mu}(m_W) = -\frac{y_S^{(1)} y_S^{*(2)}}{16\pi^2} \frac{5}{12}$  for  $S$ . All in all we find that the dipole coefficients are approximately given by

$$\begin{aligned}
 d_{e\mu}(m_W) &\simeq \frac{e}{2} \frac{v^2}{M^2} \left[ \Delta d_{e\mu}(m_W) + (C_{DW}^{e\mu}(M) - C_{DB}^{e\mu}(M)) \left( 1 - N_c y_t^2 \frac{\ln(M/m_W)}{16\pi^2} \right) \right. \\
 &\quad \left. + \left( (-N_c y_t^2 + 2\lambda) C_L^{e\mu}(M) + N_c y_t^2 C_{L3}^{e\mu}(M) - \frac{5}{8} g^2 C_y^{e\mu}(M) \right) \frac{\ln(M/m_W)}{(16\pi^2)^2} \right], \\
 d_{\mu e}(m_W) &\simeq \frac{e}{2} \frac{v^2}{M^2} \left[ \Delta d_{\mu e}(m_W) + (C_{DW}^{\mu e}(M) - C_{DB}^{\mu e}(M)) \left( 1 - N_c y_t^2 \frac{\ln(M/m_W)}{16\pi^2} \right) \right. \\
 &\quad \left. + \left( (-2N_c y_t^2 + 2\lambda) C_R^{\mu e}(M) - \frac{5}{8} g^2 C_y^{\mu e}(M) \right) \frac{\ln(M/m_W)}{(16\pi^2)^2} \right]. \tag{8.5}
 \end{aligned}$$

We should still run these coefficients from  $m_W$  to  $m_\mu$ , but we will not include these effects here as they can be found elsewhere.

Eq. (8.5) shows that the two-loop RG running can be sizable. For instance, for the singlet model  $S$ , setting the Yukawa couplings of the heavy fermions to one  $y_S^{(i)} = 1$ , the current bound on  $\mu \rightarrow e\gamma$  implies  $M \gtrsim 43$  TeV. In this case the RG contribution accounts for approximately the 20% of the total magnitude of  $d_{e\mu}$ . For the doublet  $D$  model the RG contribution has a slightly larger impact. Setting again the heavy Yukawas  $y_D^{(i)} = 1$ , we find that  $M \gtrsim 54$  TeV, with the RG contribution being a 25% of the total magnitude of  $d_{\mu e}$ . In general, for exponentially larger values of  $M$  the RG contribution would dominate, but for relatively low values of  $M$  the importance of the RG contribution is model dependent.

## 8.2 BSM with lepton universality violations

BSM sectors that couple only to the muons of the SM have been recently proposed to explain some experimental discrepancies in the muon sector. A particular possibility is the operator

$$\frac{1}{M^2} \bar{L}_L^{(2)} \tau^a \gamma^\mu L_L^{(2)} \bar{Q}_L^{(i)} \tau^a \gamma_\mu Q_L^{(i)}, \tag{8.6}$$

which could arise from integrating a heavy vector boson that only couples to muons and to the  $i$  family quarks. In the presence of this lepton universality breaking from some BSM, lepton number is not anymore automatically preserved since the diagonalization of the SM Yukawa matrix  $y_e$  leads, in the presence of eq. (8.6), to muon number violations. In particular, the operator  $\mathcal{O}_{LL3}^{\mu ett}$  is induced with

$$\frac{C_{LL3}^{\mu ett}}{\Lambda^2} = \frac{U_{LL}^{21} U_{QL}^{\dagger i3} U_{QL}^{i3}}{M^2}, \tag{8.7}$$

where  $U_{L_L, Q_L}$  is the left-handed rotation that diagonalizes  $y_e$  and  $y_u$ . If  $y_{e,u}$  are roughly symmetric, we can estimate  $U_{LL}^{21} \sim \sqrt{m_e/m_\mu}$  and  $U_{QL} \sim V_{CKM}$ . Considering the constraint on the Wilson coefficient  $C_{LL3}^{\mu ett}$  from  $\mu \rightarrow e\gamma$ , we obtain the bound

$$M \gtrsim 0.8 \text{ TeV}, \text{ for } i = 2, \quad M \gtrsim 60 \text{ TeV}, \text{ for } i = 3. \tag{8.8}$$

On the other hand, the operator (8.6) also induces a contribution to  $b \rightarrow s\mu\mu$  of order  $C_{LL3}^{\mu\mu bs}/\Lambda^2 = U_{QL}^{\dagger i2} U_{QL}^{i3}/M^2$  that is bounded from (8.8) to be

$$\frac{C_{LL3}^{\mu\mu bs}}{\Lambda^2} \lesssim \frac{1}{(4 \text{ TeV})^2}, \text{ for } i = 2, \quad \frac{C_{LL3}^{\mu\mu bs}}{\Lambda^2} \lesssim \frac{1}{(290 \text{ TeV})^2}, \text{ for } i = 3. \quad (8.9)$$

According to ref. [51], we need  $C_{LL3}^{\mu\mu bs}/\Lambda^2 \sim 1/(56 \text{ TeV})^2$  in order to explain the experimental discrepancy in  $B \rightarrow K\mu\mu$ . From eq. (8.9) we see that  $\mu \rightarrow e\gamma$  allows for the possibility  $i = 2$  but not  $i = 3$  (unless of course some of the above assumptions are relaxed).

## 9 Conclusions

In this work we have analyzed the impact of Lepton Flavor Violation processes with  $\Delta L_\mu = \Delta L_e = 1$  on the SM EFT. The most stringent constraints arise from  $\mu \rightarrow e\gamma$ ,  $\mu \rightarrow eee$  and the transition rate  $\mu N \rightarrow eN$ , where a rich program of measurements is planned in the upcoming decade as summarized in table 1. Given these spectacular prospects, our main goal here has been to understand at which loop order the different dimension-six operators of the SM EFT mix into these LFV observables. In particular, we have argued that the current and future precision reach of  $\mu \rightarrow e\gamma$  required the knowledge of operator mixings at the two-loop level.

We have shown that due to selection rules only one type of operators enter at the one-loop level into  $\mu \rightarrow e\gamma$ , and only two other types are doing it at the two-loop order.<sup>12</sup> This is sketched in figure 1. The two operators mixing into  $\mu \rightarrow e\gamma$  at the two-loop order are  $|H|^2 H\psi\psi$  and  $H^\dagger D_\mu H \bar{\psi} \gamma^\mu \psi$  which at tree level induce LFV  $h$ ,  $Z$  and  $W$  couplings. While the mixing from  $|H|^2 H\psi\psi$  was already calculated in [4, 44], we have presented here the calculation of the  $H^\dagger D_\mu H \bar{\psi} \gamma^\mu \psi$  mixing. In particular, we have calculated the two-loop anomalous dimensions of  $C_{DW,DB}^{\mu e, e\mu}$  arising from  $C_{L,L3,R}^{\mu e}$ . Our task was greatly simplified by using on-shell tools. In section 4 we provided a lightning review of the on-shell methods that we used. Then, we explained in detail the calculation of the two-loop mixings, showing how this simply reduces to a product of tree-level amplitudes integrated over some phase space. We have also analyzed the operator mixing for the  $\mu \rightarrow eee$  and  $\mu N \rightarrow eN$  observables, although in these cases we have shown that a one-loop analysis was enough.

An interesting application of our analysis has been to obtain a bound on  $(C_L^{\mu e} - C_{L3}^{\mu e})$  and  $C_y^{\mu e, e\mu}$  from  $\mu \rightarrow e\gamma$  that is competitive with bounds coming from other observables. In particular we have shown that the bound on  $C_y^{\mu e, e\mu}$  constrains  $\text{BR}(h \rightarrow \mu e)$  to be too small to be detected in future colliders. This interplay between the different bounds arising from the different LFV precision measurements was discussed in section 7, and the actual bounds were shown in table 2 where we indicated the loop order of the mixing of each operator into the process of interest.

Finally, we have shown a few illustrative examples of how to use our EFT analysis to understand the different BSM effects inducing  $\mu \rightarrow e\gamma$ . In special, we have considered

---

<sup>12</sup>There are also operators of type  $\bar{\psi}^2 \psi^2$  that enter at the two-loop level but their effects are suppressed by small Yukawa couplings.



models with heavy vector-like fermions and compared the different contributions coming from EFT matching at  $\Lambda$  and  $m_W$  with those from running.

Our main message here has been to show that the next generation of LFV precision measurements will require the knowledge of renormalization effects at higher orders, where on-shell methods have been shown to be extremely suitable not only for performing calculations, but also for understanding the patterns behind them.

## Acknowledgments

We thank Marc Riembau for early collaboration and interesting discussions. C.F. is supported by the fellowship FPU18/04733 from the Spanish Ministry of Science, Innovation and Universities. A.P. has been partly supported by the Catalan ICREA Academia Program, and grants 2014-SGR-1450, PID2020-115845GB-I00/AEI/ 10.13039/501100011033 and Severo Ochoa excellence program SEV-2016-0588.

## A One-loop anomalous dimensions relevant for LFV

In this appendix we present the one-loop anomalous dimensions of the Wilson coefficients that enter at tree level into the observables  $\mu \rightarrow e\gamma$ ,  $\mu \rightarrow eee$  and  $\mu N \rightarrow eN$ . These results can be found, for example, at [43, 52]. We are not interested in self-renormalization but only in mixing effects coming from other Wilson coefficients not present at that level. This gives us the leading order at which the coefficients enter into the LFV processes.

### A.1 $\mu \rightarrow e\gamma$

The Wilson coefficient entering at tree level into  $\mu \rightarrow e\gamma$  is the combination  $(C_{DW} - C_{DB})$ . This can only be renormalized at the one-loop level by operators with  $|h| = 2$ . In particular, the orthogonal combination  $(C_{DW} + C_{DB})$  can mix into  $(C_{DW} - C_{DB})$ . Using

$$\frac{d}{d \ln \mu} C_{DW} = \frac{1}{16\pi^2} \left[ \left( g^2 \left( -\frac{11}{12} + \frac{1}{4} t_{\theta_w}^2 \right) + N_c y_t^2 \right) C_{DW} - \frac{1}{2} g^2 t_{\theta_w} C_{DB} \right], \quad (\text{A.1})$$

$$\frac{d}{d \ln \mu} C_{DB} = \frac{1}{16\pi^2} \left[ -\frac{3}{2} g^2 t_{\theta_w} C_{DW} + \left( g^2 \left( -\frac{9}{4} + \frac{151}{12} t_{\theta_w}^2 \right) + N_c y_t^2 \right) C_{DB} \right], \quad (\text{A.2})$$

we derive this mixing to be

$$\frac{d}{d \ln \mu} (C_{DW} - C_{DB}) = \frac{g^2}{16\pi^2} \left[ \frac{2}{3} + \frac{1}{2} t_{\theta_w} - \frac{37}{6} t_{\theta_w}^2 \right] (C_{DW} + C_{DB}). \quad (\text{A.3})$$

The other  $|h| = 2$  operators are eq. (2.5). Among them, however,  $\mathcal{O}_{LeQu}$  leads to an amplitude  $\mathcal{A} \sim \langle le \rangle \langle qu \rangle$  antisymmetric under  $l \leftrightarrow e$ , so it cannot renormalize eq. (4.2) and eq. (4.3) that are symmetric under this exchange [5]. Therefore only  $\mathcal{O}_{LuQe}$  gives a nonzero contribution to the dipoles at the one-loop level (derived in detail in section 4.1):

$$\frac{d}{d \ln \mu} \begin{pmatrix} C_{DB} \\ C_{DW} \end{pmatrix} = \frac{y_u N_c}{16\pi^2} \begin{pmatrix} 5/12 \\ -1/4 \end{pmatrix} C_{LuQe}. \quad (\text{A.4})$$



There are several Wilson coefficients of eq. (2.5) however that can enter into the renormalization of  $C_{LuQe}$ . Knowing these effects allows us to understand which Wilson coefficients can renormalize the dipoles at the two-loop level with a double log. We have

$$\begin{aligned} \frac{d}{d \ln \mu} C_{LuQe}^{\mu e q q} &= \frac{-g^2}{16\pi^2} \left( 3 + 5t_{\theta_W}^2 \right) C_{LeQu}^{\mu e q q} \\ &+ \frac{4y_u}{16\pi^2} \left( C_{RR}^{\mu e u u} + \frac{y_e}{y_\mu} C_{LL}^{\mu e q q} - 3 \frac{y_e}{y_\mu} C_{LL3}^{\mu e q q} + \frac{y_e}{y_\mu} C_{LR}^{\mu e u u} + C_{RL}^{\mu e q q} \right), \end{aligned} \quad (\text{A.5})$$

$$\begin{aligned} \frac{d}{d \ln \mu} C_{LuQe}^{e \mu q q} &= \frac{-g^2}{16\pi^2} \left( 3 + 5t_{\theta_W}^2 \right) C_{LeQu}^{e \mu q q} \\ &+ \frac{4y_u}{16\pi^2} \left( \frac{y_e}{y_\mu} C_{RR}^{e \mu u u} + C_{LL}^{e \mu q q} - 3 C_{LL3}^{e \mu q q} + C_{LR}^{e \mu u u} + \frac{y_e}{y_\mu} C_{RL}^{e \mu q q} \right). \end{aligned} \quad (\text{A.6})$$

The first terms of both equations correspond to a  $|h| = 2$  operator, while the other terms correspond to  $h = 0$  operators where the helicity selection rule  $\Delta n \geq |\Delta h|$  is violated due to the Higgs interchange that leads to a contribution  $\propto y_u y_e$  [10, 11].

## A.2 $\mu \rightarrow eee$

The Wilson coefficients  $C_{L,L3}^{\mu e}$  enter in eq. (5.2) but only in the combination  $C_L^{\mu e} + C_{L3}^{\mu e}$ . For this reason it is convenient to define

$$C_{L\pm} = C_L \pm C_{L3}, \quad (\text{A.7})$$

as we are only interested in the mixing from  $C_{L-}$  into  $C_{L+}$ . From

$$\frac{d}{d \ln \mu} C_L^{\mu e} = \frac{g^2}{16\pi^2} \frac{4}{3} t_{\theta_W}^2 Y_H^2 C_L^{\mu e}, \quad \frac{d}{d \ln \mu} C_{L3}^{\mu e} = -\frac{g^2}{16\pi^2} \frac{17}{3} C_{L3}^{\mu e}, \quad (\text{A.8})$$

we obtain the mixing

$$\frac{d}{d \ln \mu} C_{L+} = \frac{g^2}{16\pi^2} \left[ \frac{17}{6} + \frac{2}{3} t_{\theta_W}^2 Y_H^2 \right] C_{L-}, \quad (\text{A.9})$$

where we neglected self-renormalization.

For the four-fermion  $\mu eee$  Wilson coefficients entering into eq. (5.2), we have

$$\begin{aligned} \frac{d}{d \ln \mu} C_{LL}^{\mu eee} &= \frac{g^2}{16\pi^2} \left\{ \frac{4}{3} Y_{L_L} t_{\theta_W}^2 \left[ N_c \left( 2Y_{Q_L} C_{LL}^{\mu e q q} + Y_{u_R} C_{LR}^{\mu e u u} + Y_{d_R} C_{LR}^{\mu e d d} \right) + Y_H C_L^{\mu e} \right] \right. \\ &\quad \left. + \frac{2N_c C_{LL3}^{\mu e q q}}{3} + \frac{C_{L3}^{\mu e}}{3} \right\}, \\ \frac{d}{d \ln \mu} C_{RR}^{\mu eee} &= \frac{g^2}{16\pi^2} \frac{4}{3} Y_{e_R} t_{\theta_W}^2 \left[ N_c \left( 2Y_{Q_L} C_{RL}^{\mu e q q} + Y_{u_R} C_{RR}^{\mu e u u} + Y_{d_R} C_{RR}^{\mu e d d} \right) \right], \\ \frac{d}{d \ln \mu} C_{LR}^{\mu eee} &= \frac{g^2}{16\pi^2} \frac{4}{3} Y_{e_R} t_{\theta_W}^2 \left[ N_c \left( 2Y_{Q_L} C_{LL}^{\mu e q q} + Y_{u_R} C_{LR}^{\mu e u u} + Y_{d_R} C_{LR}^{\mu e d d} \right) + Y_H C_L^{\mu e} \right], \\ \frac{d}{d \ln \mu} C_{RL}^{\mu eee} &= \frac{g^2}{16\pi^2} \frac{4}{3} Y_{L_L} t_{\theta_W}^2 \left[ N_c \left( 2Y_{Q_L} C_{RL}^{\mu e q q} + Y_{u_R} C_{RR}^{\mu e u u} + Y_{d_R} C_{RR}^{\mu e d d} \right) \right], \end{aligned} \quad (\text{A.10})$$

where we are interested in the case where  $q, u, d$  corresponds to the 2nd and 3rd family, since for the 1st family these Wilsons are already highly constrained at tree level by  $\mu N \rightarrow eN$ . Also we are interested in the projection  $C_L \rightarrow C_{L-}/2$  and  $C_{L3} \rightarrow -C_{L-}/2$ . The renormalization from  $C_{LL,LL3,RR,LR,RL}^{\mu e \tau \tau}$  can be obtained from eq. (A.10) by the replacement  $q, d \rightarrow \tau$ ,  $N_c \rightarrow 1$ ,  $Y_{Q_L} \rightarrow Y_{L_L}$ ,  $Y_{d_R} \rightarrow Y_{e_R}$ , and putting to zero the contribution from  $u$ .

### A.3 $\mu N \rightarrow eN$

The relevant anomalous dimensions of the Wilson coefficients  $C_{LL,RR,LR,RL}^{\mu e u u}$  of eq. (6.4) can be obtained from those in eq. (A.10) by the replacements  $Y_{L_L} \rightarrow Y_{Q_L}$  and  $Y_{e_R} \rightarrow Y_{u_R}$ .

## B Conventions and minimal form factors

For the computations in section 4, we work with 2-component Weyl spinors, and take all fermion fields to be right-handed. Then the SM dimension-four Lagrangian is

$$\begin{aligned} \mathcal{L}_4 = & (D^\mu H^\dagger)(D_\mu H) - \lambda(|H|^2 - v^2/2)^2 \\ & + \sum_{\psi=Q,L,u,d,e} \psi^\dagger \bar{\sigma}^\mu D_\mu \psi - y_u \delta_i^j H_j^\dagger Q^i u - y_d \epsilon_{ij} H^j Q^i d - y_e \epsilon_{ij} H^j L^i e, \end{aligned} \quad (\text{B.1})$$

where  $i, j = 1, 2$  upper (lower) indices of the (anti-)fundamental representation of  $SU(2)$ . All other indices like Lorentz, families etc. are contracted properly but not shown. We define  $\sigma^\mu = (1, \vec{\sigma})$  and  $\bar{\sigma}^\mu = (1, -\vec{\sigma})$ . The covariant derivatives are  $D_\mu = \partial_\mu - ig(\tau^\alpha/2)A_\mu^\alpha - ig'YB_\mu$ , where  $\tau^\alpha$  are Pauli matrices and  $Y$  is the hypercharge.

Next we report the minimal form factors in both 4-component Dirac and 2-component Weyl fermions. Remember that they are Fourier transforms of position-space form factors evaluated at zero momentum, as defined in the text. Starting with the dipole operators:

$$\begin{aligned} F_{\mathcal{O}_{DB}^{e\mu}} &= \langle 1_{L_k}^- 2_e^- 3_{H_m} 4_B^- | \bar{L}_{L,i}^{(1)} \Sigma^{\mu\nu} e_R^{(2)} H^j \delta_j^i B_{\mu\nu} | 0 \rangle = \langle 1_k^- 2^- 3_m 4^- | E^i \sigma^{\mu\nu} \mu H^j \epsilon_{ij} B_{\mu\nu} | 0 \rangle \\ &= 2\sqrt{2} \langle 14 \rangle \langle 42 \rangle \epsilon_{km}, \end{aligned} \quad (\text{B.2})$$

$$\begin{aligned} F_{\mathcal{O}_{DW}^{e\mu}} &= \langle 1_{L_k}^- 2_e^- 3_{H_m} 4_{W_\beta}^- | \bar{L}_{L,i}^{(1)} (\tau^\alpha)_j^i \Sigma^{\mu\nu} e_R^{(2)} H^j W_{\mu\nu}^\alpha | 0 \rangle \\ &= \langle 1_k^- 2^- 3_m 4_\beta^- | E^i \epsilon_{ii'} (\tau^\alpha)_j^{i'} \sigma^{\mu\nu} \mu H^j W_{\mu\nu}^\alpha | 0 \rangle \\ &= 2\sqrt{2} \langle 14 \rangle \langle 42 \rangle \epsilon_{kk'} (\tau^\beta)_m^{k'}, \end{aligned} \quad (\text{B.3})$$

where  $\Sigma^{\mu\nu} = \frac{i}{2}[\gamma^\mu, \gamma^\nu]$  such that  $(\bar{\psi}_L \Sigma^{\mu\nu} \psi_R)^\dagger = \bar{\psi}_R \Sigma^{\mu\nu} \psi_L$ . Similarly in 2-component Weyl basis we define  $\sigma^{\mu\nu} = \frac{i}{2}(\sigma^\mu \bar{\sigma}^\nu - \sigma^\nu \bar{\sigma}^\mu)$ . The relation between conjugated fermion doublets in Dirac and Weyl is  $L^i = C \cdot \epsilon^{ij} \cdot L_{L,j}^*$  where  $C$  is acting on Lorentz indices and  $\epsilon = i\tau_2$

acting on SU(2) indices. Next, the current-current operators:

$$\begin{aligned}
 F_{\mathcal{O}_L^{e\mu}} &= \langle 1_{L_k}^- 2_{L_l}^+ 3_{H_m} 4_{H_n}^* | \bar{L}_L^{(1)} \gamma^\mu L_L^{(2)} H^\dagger i \overleftrightarrow{\partial}_\mu H | 0 \rangle = \langle 2_l^+ 1_k^- 3_m 4_n^* | -M^\dagger \bar{\sigma}^\mu E H^\dagger i \overleftrightarrow{\partial}_\mu H | 0 \rangle \\
 &= 2 \langle 13 \rangle [32] (-\delta_l^k \delta_m^n), \tag{B.4}
 \end{aligned}$$

$$\begin{aligned}
 F_{\mathcal{O}_{L3}^{e\mu}} &= \langle 1_{L_k}^- 2_{L_l}^+ 3_{H_m} 4_{H_n}^* | \bar{L}_L^{(1)} \gamma^\mu \tau^\alpha L_L^{(2)} H^\dagger i \overleftrightarrow{\partial}_\mu H | 0 \rangle = \langle 2_l^+ 1_k^- 3_m 4_n^* | -M^\dagger \bar{\sigma}^\mu (-\tau^\alpha) E H^\dagger i \overleftrightarrow{\partial}_\mu H | 0 \rangle \\
 &= 2 \langle 13 \rangle [32] (\tau^\alpha)_l^k (\tau^\alpha)_m^n, \tag{B.5}
 \end{aligned}$$

$$\begin{aligned}
 F_{\mathcal{O}_R^{e\mu}} &= \langle 1_e^+ 2_e^- 3_{H_m} 4_{H_n}^* | \bar{e}_R^{(1)} \gamma^\mu e_R^{(2)} H^\dagger i \overleftrightarrow{\partial}_\mu H | 0 \rangle = \langle 1^+ 2^- 3_m 4_n^* | e^\dagger \bar{\sigma}^\mu \mu H^\dagger i \overleftrightarrow{\partial}_\mu H | 0 \rangle \\
 &= 2 [13] \langle 32 \rangle \delta_m^n, \tag{B.6}
 \end{aligned}$$

where to distinguish the lepton flavor, we used letters  $E$  and  $e$  for electron doublet and singlet respectively, and  $M$  and  $\mu$  for muon.

### C Tensors

Here we give the SU(2) tensors used in the main text to compute the anomalous dimensions:

$\mathcal{C}_{kc}^{ab} \times \mathcal{D}_{bla}^c$	$\mathcal{O}_L$	$\mathcal{O}_{L3}$
$\mathcal{O}_{DB}$	$g' \cdot 2 \delta_k^a \delta_c^b \times (-\delta_b^c \delta_l^a) \epsilon_{l'a}$	$g' \cdot 2 \delta_k^a \delta_c^b \times (\tau^\beta)_b^c (\tau^\beta)_l^a \epsilon_{l'a}$
$\mathcal{O}_{DW}$	$g \cdot 2 (\tau^\alpha/2)_k^a \delta_c^b \times (-\delta_b^c \delta_l^a) \epsilon_{l'a}$	$g \cdot 2 (\tau^\alpha/2)_k^a \delta_c^b \times (\tau^\beta)_b^c (\tau^\beta)_l^a \epsilon_{l'a}$

(C.1)

$\mathcal{F}_{akc}^b \times \mathcal{G}_{bl}^{ca}$	$\mathcal{O}_L$	$\mathcal{O}_{L3}$
$\mathcal{O}_{DB}$	$2(\delta_k^b \epsilon_{ac} + \delta_c^b \epsilon_{ak}) \times g' (-\delta_b^c \delta_l^a)$	$2(\delta_k^b \epsilon_{ac} + \delta_c^b \epsilon_{ak}) \times g' (\tau^\beta)_b^c (\tau^\beta)_l^a$
$\mathcal{O}_{DW}$	$2(\delta_k^b \epsilon_{ac} + \delta_c^b \epsilon_{ak}) \times g (-\tau^\alpha/2)_b^c \delta_l^a$	$2(\delta_k^b \epsilon_{ac} + \delta_c^b \epsilon_{ak}) \times g (\tau^\alpha/2)_{b'}^c (\tau^\beta)_{b'}^c (\tau^\beta)_l^a$

(C.2)

while for the  $\mathcal{O}_R$  operator:

$\mathcal{C}_{kc}^{ab} \times \mathcal{D}_{bla}^c$	$\mathcal{O}_R$	$\mathcal{F}_{lkc}^b \times \mathcal{G}_b^c$	$\mathcal{O}_R$
$\mathcal{O}_{DB}$	$g' \cdot 2 \delta_k^a \delta_c^b \times \delta_b^c \delta_l^a \epsilon_{l'a}$	$\mathcal{O}_{DB}$	$2(\delta_k^b \epsilon_{lc} + \delta_c^b \epsilon_{lk}) \times g' \delta_b^c$
$\mathcal{O}_{DW}$	$g \cdot 2 (\tau^\alpha/2)_k^a \delta_c^b \times \delta_b^c \delta_l^a \epsilon_{l'a}$	$\mathcal{O}_{DW}$	$2(\delta_k^b \epsilon_{lc} + \delta_c^b \epsilon_{lk}) \times g (\tau^\alpha/2)_b^c$

(C.3)

We emphasize that for  $\mathcal{O}_L$  and  $\mathcal{O}_{L3}$  these tensors should be used in (4.28), (4.29) and (4.31), (4.32), while for  $\mathcal{O}_R$  they should be used in (4.28), (4.36) and (4.37), (4.38).

**Open Access.** This article is distributed under the terms of the Creative Commons Attribution License ([CC-BY 4.0](https://creativecommons.org/licenses/by/4.0/)), which permits any use, distribution and reproduction in any medium, provided the original author(s) and source are credited.

## References

- [1] L. Calibbi and G. Signorelli, *Charged Lepton Flavour Violation: An Experimental and Theoretical Introduction*, *Riv. Nuovo Cim.* **41** (2018) 71 [[arXiv:1709.00294](#)] [[INSPIRE](#)].
- [2] A. Baldini et al., *A submission to the 2020 update of the European Strategy for Particle Physics on behalf of the COMET, MEG, Mu2e and Mu3e collaborations*, [arXiv:1812.06540](#) [[INSPIRE](#)].
- [3] S. Caron-Huot and M. Wilhelm, *Renormalization group coefficients and the S-matrix*, *JHEP* **12** (2016) 010 [[arXiv:1607.06448](#)] [[INSPIRE](#)].
- [4] J. Elias Miró, J. Ingoldby and M. Riembau, *EFT anomalous dimensions from the S-matrix*, *JHEP* **09** (2020) 163 [[arXiv:2005.06983](#)] [[INSPIRE](#)].
- [5] P. Baratella, C. Fernandez and A. Pomarol, *Renormalization of Higher-Dimensional Operators from On-shell Amplitudes*, *Nucl. Phys. B* **959** (2020) 115155 [[arXiv:2005.07129](#)] [[INSPIRE](#)].
- [6] M. Jiang, T. Ma and J. Shu, *Renormalization Group Evolution from On-shell SMEFT*, *JHEP* **01** (2021) 101 [[arXiv:2005.10261](#)] [[INSPIRE](#)].
- [7] Z. Bern, J. Parra-Martinez and E. Sawyer, *Structure of two-loop SMEFT anomalous dimensions via on-shell methods*, *JHEP* **10** (2020) 211 [[arXiv:2005.12917](#)] [[INSPIRE](#)].
- [8] P. Baratella, D. Haslehner, M. Ruhdorfer, J. Serra and A. Weiler, *RG of GR from on-shell amplitudes*, *JHEP* **03** (2022) 156 [[arXiv:2109.06191](#)] [[INSPIRE](#)].
- [9] M. Accettulli Huber and S. De Angelis, *Standard Model EFTs via on-shell methods*, *JHEP* **11** (2021) 221 [[arXiv:2108.03669](#)] [[INSPIRE](#)].
- [10] J. Elias-Miro, J.R. Espinosa and A. Pomarol, *One-loop non-renormalization results in EFTs*, *Phys. Lett. B* **747** (2015) 272 [[arXiv:1412.7151](#)] [[INSPIRE](#)].
- [11] C. Cheung and C.-H. Shen, *Nonrenormalization Theorems without Supersymmetry*, *Phys. Rev. Lett.* **115** (2015) 071601 [[arXiv:1505.01844](#)] [[INSPIRE](#)].
- [12] Z. Bern, J. Parra-Martinez and E. Sawyer, *Nonrenormalization and Operator Mixing via On-Shell Methods*, *Phys. Rev. Lett.* **124** (2020) 051601 [[arXiv:1910.05831](#)] [[INSPIRE](#)].
- [13] N. Craig, M. Jiang, Y.-Y. Li and D. Sutherland, *Loops and Trees in Generic EFTs*, *JHEP* **08** (2020) 086 [[arXiv:2001.00017](#)] [[INSPIRE](#)].
- [14] M. Jiang, J. Shu, M.-L. Xiao and Y.-H. Zheng, *Partial Wave Amplitude Basis and Selection Rules in Effective Field Theories*, *Phys. Rev. Lett.* **126** (2021) 011601 [[arXiv:2001.04481](#)] [[INSPIRE](#)].
- [15] P. Baratella, C. Fernandez, B. von Harling and A. Pomarol, *Anomalous Dimensions of Effective Theories from Partial Waves*, *JHEP* **03** (2021) 287 [[arXiv:2010.13809](#)] [[INSPIRE](#)].
- [16] H.-L. Li, J. Shu, M.-L. Xiao and J.-H. Yu, *Depicting the Landscape of Generic Effective Field Theories*, [arXiv:2012.11615](#) [[INSPIRE](#)].
- [17] J. Shu, M.-L. Xiao and Y.-H. Zheng, *Constructing general partial waves and renormalization in EFT*, [arXiv:2111.08019](#) [[INSPIRE](#)].
- [18] Y. Shadmi and Y. Weiss, *Effective Field Theory Amplitudes the On-Shell Way: Scalar and Vector Couplings to Gluons*, *JHEP* **02** (2019) 165 [[arXiv:1809.09644](#)] [[INSPIRE](#)].
- [19] G. Durieux, T. Kitahara, Y. Shadmi and Y. Weiss, *The electroweak effective field theory from on-shell amplitudes*, *JHEP* **01** (2020) 119 [[arXiv:1909.10551](#)] [[INSPIRE](#)].

- [20] G. Durieux and C.S. Machado, *Enumerating higher-dimensional operators with on-shell amplitudes*, *Phys. Rev. D* **101** (2020) 095021 [[arXiv:1912.08827](#)] [[INSPIRE](#)].
- [21] Z.-Y. Dong, T. Ma and J. Shu, *Constructing on-shell operator basis for all masses and spins*, [arXiv:2103.15837](#) [[INSPIRE](#)].
- [22] A. Crivellin, S. Najjari and J. Rosiek, *Lepton Flavor Violation in the Standard Model with general Dimension-Six Operators*, *JHEP* **04** (2014) 167 [[arXiv:1312.0634](#)] [[INSPIRE](#)].
- [23] G.M. Pruna and A. Signer, *The  $\mu \rightarrow e\gamma$  decay in a systematic effective field theory approach with dimension 6 operators*, *JHEP* **10** (2014) 014 [[arXiv:1408.3565](#)] [[INSPIRE](#)].
- [24] G.M. Pruna and A. Signer, *Lepton-flavour violating decays in theories with dimension 6 operators*, *EPJ Web Conf.* **118** (2016) 01031 [[arXiv:1511.04421](#)] [[INSPIRE](#)].
- [25] A. Crivellin, S. Davidson, G.M. Pruna and A. Signer, *Renormalisation-group improved analysis of  $\mu \rightarrow e$  processes in a systematic effective-field-theory approach*, *JHEP* **05** (2017) 117 [[arXiv:1702.03020](#)] [[INSPIRE](#)].
- [26] M. Ardu and S. Davidson, *What is Leading Order for LFV in SMEFT?*, *JHEP* **08** (2021) 002 [[arXiv:2103.07212](#)] [[INSPIRE](#)].
- [27] S. Davidson, *Completeness and complementarity for  $\mu \rightarrow e\gamma$ ,  $\mu \rightarrow e\bar{e}e$  and  $\mu A \rightarrow eA$* , *JHEP* **02** (2021) 172 [[arXiv:2010.00317](#)] [[INSPIRE](#)].
- [28] S. Davidson,  *$\mu \rightarrow e\gamma$  and matching at  $m_W$* , *Eur. Phys. J. C* **76** (2016) 370 [[arXiv:1601.07166](#)] [[INSPIRE](#)].
- [29] A. Celis, V. Cirigliano and E. Passemar, *Lepton flavor violation in the Higgs sector and the role of hadronic  $\tau$ -lepton decays*, *Phys. Rev. D* **89** (2014) 013008 [[arXiv:1309.3564](#)] [[INSPIRE](#)].
- [30] A. Celis, V. Cirigliano and E. Passemar, *Model-discriminating power of lepton flavor violating  $\tau$  decays*, *Phys. Rev. D* **89** (2014) 095014 [[arXiv:1403.5781](#)] [[INSPIRE](#)].
- [31] T. Husek, K. Monsalvez-Pozo and J. Portoles, *Lepton-flavour violation in hadronic tau decays and  $\mu - \tau$  conversion in nuclei*, *JHEP* **01** (2021) 059 [[arXiv:2009.10428](#)] [[INSPIRE](#)].
- [32] V. Cirigliano, K. Fuyuto, C. Lee, E. Mereghetti and B. Yan, *Charged Lepton Flavor Violation at the EIC*, *JHEP* **03** (2021) 256 [[arXiv:2102.06176](#)] [[INSPIRE](#)].
- [33] MEG collaboration, *Search for the lepton flavour violating decay  $\mu^+ \rightarrow e^+\gamma$  with the full dataset of the MEG experiment*, *Eur. Phys. J. C* **76** (2016) 434 [[arXiv:1605.05081](#)] [[INSPIRE](#)].
- [34] SINDRUM collaboration, *Search for the Decay  $\mu^+ \rightarrow e^+e^+e^-$* , *Nucl. Phys. B* **299** (1988) 1 [[INSPIRE](#)].
- [35] SINDRUM II collaboration, *A Search for muon to electron conversion in muonic gold*, *Eur. Phys. J. C* **47** (2006) 337 [[INSPIRE](#)].
- [36] ATLAS collaboration, *Search for the Higgs boson decays  $H \rightarrow ee$  and  $H \rightarrow e\mu$  in  $pp$  collisions at  $\sqrt{s} = 13$  TeV with the ATLAS detector*, *Phys. Lett. B* **801** (2020) 135148 [[arXiv:1909.10235](#)] [[INSPIRE](#)].
- [37] MEG II collaboration, *The design of the MEG II experiment*, *Eur. Phys. J. C* **78** (2018) 380 [[arXiv:1801.04688](#)] [[INSPIRE](#)].
- [38] A. Blondel et al., *Research Proposal for an Experiment to Search for the Decay  $\mu \rightarrow eee$* , [arXiv:1301.6113](#) [[INSPIRE](#)].

- [39] MU2E collaboration, *Mu2e Technical Design Report*, [arXiv:1501.05241](#) [INSPIRE].
- [40] B. Grzadkowski, M. Iskrzynski, M. Misiak and J. Rosiek, *Dimension-Six Terms in the Standard Model Lagrangian*, *JHEP* **10** (2010) 085 [[arXiv:1008.4884](#)] [INSPIRE].
- [41] J. Elias-Miro, J.R. Espinosa, E. Masso and A. Pomarol, *Higgs windows to new physics through  $d = 6$  operators: constraints and one-loop anomalous dimensions*, *JHEP* **11** (2013) 066 [[arXiv:1308.1879](#)] [INSPIRE].
- [42] Y. Kuno and Y. Okada, *Muon decay and physics beyond the standard model*, *Rev. Mod. Phys.* **73** (2001) 151 [[hep-ph/9909265](#)] [INSPIRE].
- [43] E.E. Jenkins, A.V. Manohar and M. Trott, *Renormalization Group Evolution of the Standard Model Dimension Six Operators II: Yukawa Dependence*, *JHEP* **01** (2014) 035 [[arXiv:1310.4838](#)] [INSPIRE].
- [44] G. Panico, A. Pomarol and M. Riembau, *EFT approach to the electron Electric Dipole Moment at the two-loop level*, *JHEP* **04** (2019) 090 [[arXiv:1810.09413](#)] [INSPIRE].
- [45] R. Britto, F. Cachazo and B. Feng, *New recursion relations for tree amplitudes of gluons*, *Nucl. Phys. B* **715** (2005) 499 [[hep-th/0412308](#)] [INSPIRE].
- [46] R. Britto, F. Cachazo, B. Feng and E. Witten, *Direct proof of tree-level recursion relation in Yang-Mills theory*, *Phys. Rev. Lett.* **94** (2005) 181602 [[hep-th/0501052](#)] [INSPIRE].
- [47] K. Risager, *A Direct proof of the CSW rules*, *JHEP* **12** (2005) 003 [[hep-th/0508206](#)] [INSPIRE].
- [48] R. Kitano, M. Koike and Y. Okada, *Detailed calculation of lepton flavor violating muon electron conversion rate for various nuclei*, *Phys. Rev. D* **66** (2002) 096002 [Erratum *ibid.* **76** (2007) 059902] [[hep-ph/0203110](#)] [INSPIRE].
- [49] W. Dekens, E.E. Jenkins, A.V. Manohar and P. Stoffer, *Non-perturbative effects in  $\mu \rightarrow e\gamma$* , *JHEP* **01** (2019) 088 [[arXiv:1810.05675](#)] [INSPIRE].
- [50] A. Freitas, J. Lykken, S. Kell and S. Westhoff, *Testing the Muon  $g-2$  Anomaly at the LHC*, *JHEP* **05** (2014) 145 [Erratum *ibid.* **09** (2014) 155] [[arXiv:1402.7065](#)] [INSPIRE].
- [51] C. Cornella, D.A. Faroughy, J. Fuentes-Martin, G. Isidori and M. Neubert, *Reading the footprints of the  $B$ -meson flavor anomalies*, *JHEP* **08** (2021) 050 [[arXiv:2103.16558](#)] [INSPIRE].
- [52] R. Alonso, E.E. Jenkins, A.V. Manohar and M. Trott, *Renormalization Group Evolution of the Standard Model Dimension Six Operators III: Gauge Coupling Dependence and Phenomenology*, *JHEP* **04** (2014) 159 [[arXiv:1312.2014](#)] [INSPIRE].